1. Introduction

1.1. Literature Review

The literature review for this project is contained in the thesis written by Kelly Wilson [Reference 3]. Anyone interested in the relevant literature should consult that thesis. It was felt that any literature review would repeat the information on this subject from that thesis to this.

1.2. General Project Introduction

This is the second part of a larger project originally scheduled to be completed in three parts. The goal of the complete project is to determine the fatigue life for saline filled mammary prosthesis using a combination of computational Finite Element Analysis (FEA) and mechanical fatigue testing. The first part of this project was to define the problem, conduct mechanical testing to obtain the linear stress-strain properties of the implant material, and to develop a linear elastic two-dimensional axisymmetric FEA model. The second part of the project was to test the mechanical properties (stress-strain) of the implant material, development of nonlinear material models, integrate nonlinear material models into the two-dimensional axisymmetric FEA analysis, and generate three-dimensional FEA models. The final part of the proposed project was to develop of the stress-life (S-N) curve for the implant shell material utilizing mechanical fatigue testing, and to calculate a fatigue life of the mammary prostheses given a loading spectra and the FEA results. Another researcher performed the first section of the project, while the third section of the project has not been started.

In the second part of the project the two-dimensional axisymmetric models were extended to include nonlinear material models and some additional symmetric and three-dimensional analysis was performed. This led to the conclusion that certain regions of the implant had stresses in the shell that are compressive. It is believed these compressive stresses may cause buckling of the implant wall causing "fold flaws" to form and lead to premature failure of the implants. In the event that buckling of the implant wall does occur, the silicone elastomeric membrane would fold back on itself. The resulting fold would then allow for the implant to abrade against itself reducing the cross-sectional area of the implant wall, increasing the axial stresses, eventual leading to rupture. After the possibility of buckling was realized, an axisymmetric fold model was developed to investigate the stress concentration that would be present in the fold.

The development of the three dimensional models was hampered by the lack of a post implantation prosthesis geometry. Without the initial prosthesis geometry, there is no accurate starting point from which a three-dimensional model of the implant can be developed. The time originally scheduled for the three-dimensional analysis was instead spent expanding the two-dimensional axisymmetric FEA models including the fold model development.

The following general introductory sections are intended for a very brief introduction to the material models (section 1.2), finite element analysis (section 1.3), and fatigue (section 1.4). The determination of stress-strain properties is included in Section 2, the FEA modeling work is presented in Section 3, while Section 4 is a general overview of fatigue life prediction which is included because some initial work on fatigue life testing was conducted, though no meaningful data was completed.

1.3. Materials introduction

Engineering materials are characterized so that the mechanical deformation response of an object can be estimated. Whether the estimated response is a fatigue life calculation, internal stress analysis, or computation of a deformed geometry; the first step in computing the response is characterization of the materials. The characteristics that need to be determined depend on the type of investigation that is being performed. If the internal stresses or a deformed geometry analysis is performed, then the stress-strain properties of the material must be determined. If a fatigue life estimate is to be calculated, then stress versus cycles to failure properties are needed. In any solids analysis, the starting point for the material characterization is mechanical testing. Using the test data, a mathematical trend model of the materials behavior is generated, in an attempt to eliminate testing each case.

The mechanical testing needs to be conducted in a way that will yield useful material characteristics, meaning that the tests must be representative of the expected loads. For example if an analysis is to determine how a material will behave in compression, the test data used to generate the material formulation must be from compression testing. The need to test a material in a similar manner to that expected in the service life is critical, especially in fatigue characterization. If the fatigue characteristics are generated from data that does not resemble the service life loads, then the fatigue life estimate will be invalid and life predictions could be greatly overestimated or underestimated. In terms of this research project, fatigue testing of a folded implant specimen would be crucial. At this time there was some limited fatigue testing

conducted, however the parameters for controlling the fatigue-testing machine have not been fully determined.

All of the testing was conducted in uniaxial tension, which yielded sufficient data about how the implant material responds to loads to allow for material modeling of the implant shell material. It may be beneficial after uniaxial testing to extend the testing to multiple axes for materials like the silicone implant material. This would allow for more accurate FEA models, since the material definition would be more accurate.

Fatigue life characterization is much more difficult than material response modeling. The reason that fatigue modeling is more complicated is the number of tests that need to be conducted, all with similar precision. In most cases multiple fatigue tests need to be run at each stress level, so that a statistical fatigue life can be computed for each internal stress amplitude. And to estimate the fatigue life for any internal stress, many different stress levels need to be tested. This means that to fully characterize a materials fatigue life, hundreds of tests could be required. In fatigue testing either an applied displacement (strain) or load (stress) is selected to control the fatigue tests, and the number of cycles to failure is recorded. If the fatigue test is strain or displacement controlled, then the average stress applied to the specimen is estimated, this estimation is not required for stress or load controlled testing. After a number of samples have been stressed to a failure criterion at various applied stress levels, a fatigue life or stress versus cycles to failure (S-N) curve is generated.

1.4. FEA introduction

In this project the FEA models are being used to estimate the internal stresses and deformation that the implant and tissue experience under a prescribed load configuration.

There are three components that are required to allow for the stress and displacement approximation. These include the material formulation for all of the materials that make up the system, the definition of the initial geometry of all components of the system, and determination of the load, displacement, and mixed boundary conditions acting upon the system. Each of these components is an approximation of the real properties of the objects that make up the system, which help to simplify the real system, so that a numerical solution can be computed.

Since the method of determining the stress-strain relationship has already been briefly covered, the next simplification that must be discussed is approximating the initial geometry. The initial geometry is an estimation of the real implant and tissue geometry when not loaded. The estimated geometry is then discretized, into elements through an element meshing routine. These elements are connected together at nodal locations. This simplification was accomplished by using PATRAN, into which the initial geometry of the implant and tissue was inserted, and the meshing routine of the program was used to discretize the domain that describes both the implant and tissue geometry.

The final component of an FEA model is the definition of boundary conditions. There are three basic types of boundary conditions in an FEA model, the first is a boundary condition on displacement, the second is a load boundary condition, the final type of boundary condition is mixed, meaning that in one direction there is a displacement boundary condition while in another direction other there is a load boundary condition. A displacement boundary condition is used to indicate a fixed prescribed displacement. A load boundary condition is used to indicate a load, either as a

point force, distributed force, contact force, frictional force, etc. All boundary conditions are assigned to nodal locations, and are satisfied only at the nodal location.

All of the FEA solutions in this project were conducted using a solution technique to solve large deformation and nonlinear geometry problems. This technique involves ramping the forces applied to the model slowly over a series of steps. This type of solution is required because of the large deformation, material stiffness changes with deformation, and the nonlinear geometry`. By making a series of small time steps, all of these changes are small and can be calculated through these linear steps. The step size is related to the force applied, and the solution must converge at each step. With convergence at a step the step is incremented, and this process is repeated until the maximum applied force is reached. If the step does not converge, the step size is reduced and that step is run again, until certain non-convergence parameters are reached which exits the FEA analysis.

The FEA model now has all of the required components for a solution to be generated, but these components need to be linked in a logical manner before the solution can be computed. The basic equation used in an FEA model is {F} = [K]{x}, where {F} is a force vector, [K] is a stiffness matrix, and {x} is a displacement vector. The boundary conditions are inserted into the appropriate vector, and the stiffness matrix is computed. The types of element, combined with the material formulation of the object are used to compute the stiffness matrix. If the boundary conditions have been applied correctly, then the FEA model is fully defined, therefore, the forces and displacements at each node in the model can be computed. The computed forces can be transformed into stress using the relation that $\sigma_i = \frac{P_i}{A_i}$, where σ is the axial or shear stress in the element,

P is the axial or shear force acting on the element, and A is the cross-sectional area of that element. The force acting upon the element is computed in the FEA solutionand since the type of element that has been used is stored, along with the node locations, so the area of the element can be computed. Strain can be computed one of two ways, typically strain is computed using the stress-strain relationship, since the stress is easily typically determined in the FEA analysis, but strain can also be computed using $\varepsilon = (l_f - l_i)/l_i$, where ε is the elemental strain, l_f is the final elemental length, and l_i is the initial elemental length. Since the stress and strain are computed at each nodal location, and assuming that the mesh is well generated, then with some interpolation, the stress or strain at any point in the body is easily determined.

1.5. Fatigue introduction

Understanding the fatigue of the mammary prosthesis is the ultimate goal of this project, though the actual calculation of an estimated fatigue life can not be completed at this time, primarily because no stress-life curve was developed for the breast implant material. However, it is critical to this project to understand the steps that are required to complete the fatigue analysis.

The first step to understanding the fatigue calculation is to understand the information that is needed to perform these calculation. To develop a fatigue estimate the internal stresses of the object must be determined. Then the stress-life curve is required for the fatigue estimate. This curve is a plot of mechanical test data, where the normalized stress amplitude that was applied to the material is placed on the ordinate, while the number of cycles that are required to induce a failure as prescribed in the test are plotted on the abscissa. The loading spectra that is applied on average to the object

that the fatigue life estimate is being computed for is the final piece of required information.

The loads in the spectra are analyzed so that the internal stresses are computed. As with mammary prosthesis, the implant shell material would be tested, as opposed to testing the entire prosthesis. Once the internal stresses are known, the internal stresses are cross-referenced on the fatigue-life curve for a given stress, to generate a number of cycles at that stress until failure should occur. The ratio of the number of cycles a load is reached in the spectra to number of cycles to failure is computed. Using the Palmgren-Miner rule the fatigue life is estimated. The damage ratio for a single stress is determined using the stress to number of cycles to failure (S-N) curve and the loading spectra. The sum of the damage ratios is computed along with the number of times the spectra can be repeated is determined. The number of times the spectra can repeat determines the fatigue estimate of the object, since the time span of the loading spectra is determined with the loading spectra.

1.6. Conclusions

There were two observations, which are considered primary; the first is that compressive stresses in the shell of the implant lead to the possibility of local buckling, and the possible increase in stress due to the buckling. The second is the belief that damage may be caused during implant installation. Depending on the implantation technique that is utilized, damage or a damage increasing flaw could be introduced to the implants. Once damage or a flaw has been introduced, there is no repair method, so the nature of this damage and the flaws caused during implantation needs to be investigated.

There are a number of concerns, which need to be addressed. One is the nonlinear tissue material formulation, which is unstable and needs to be verified using mechanical testing. The second concern is the implant's initial geometry, which has not been determined with any accuracy. The third concern that needs to be investigated is how to apply time varying loads to the models, allowing for dynamic analysis. Determination of the actual loading on the outside of the body is also a concern that needs to be overcome. The final and most important difficulty that needs to be overcome is the development of a three-dimensional model, which will require all of the modeling concerns to be addressed.

2. Material Properties

2.1. General Material Properties

There are two different solid materials that need to be modeled for the stress approximation to be performed via FEA. The first of these materials is the breast tissue and the second material is the silicone membrane of the implant itself. Both of these materials had linear and nonlinear material formulations developed through mechanical testing to describe the stress-strain relationship of the respective material. A linear relationship was used to generate the FEA model, and to determine a baseline for the analysis, as well as to determine if there is any gain in accuracy or a significant penalty in computing speed using the nonlinear material formulations for the implant or tissue. The nonlinear relationships were also used to better estimate the internal stresses in the implant, and to determine if linear material formulations provide enough information about the internal stresses to give a reasonable result for the fatigue life estimate.

The linear material models for each solid material use Young's Modulus of elasticity to determine the axial stresses. The nonlinear material model for the breast tissue uses a power law formulation, while the implant nonlinear material model takes the form of a hyperelastic material model.

There is also a need to model the saline fluid that is used to fill the implants. For the FEA analysis the only required property for the saline is the fluid density. Since the density of medical saline is not significantly different from the density of water, the density for the saline fluid model was assumed to be identical to the density of water.

2.1.1 General Breast Tissue Formulation

Breast tissue is very complex, since it is actually a composite of many different tissues at varying orientations. These tissues are elastin and collagen which form connective tissues and ligaments; fatty tissues; and duct tissues. To develop an FEA model that would account for each of these tissue types would be geometrically much to complex and specific to be used in the FEA models. To simplify the breast tissue material formulation, it was assumed that the tissue would behave as a single entity, with homogeneous material properties.

2.1.1.1. Axial stress-strain relationship

The axial stress-strain relationship for the linear breast tissue material formulation was developed during the first phase of this project. Young's modulus for the breast tissue was computed based on knowing the axial material characteristics for elastin and collagen, and estimating the volumetric relationship between the two. This assumption was made because no breast tissue was available for mechanical testing and no reference could be found for breast tissue data. The elastic modulus used in the linear breast tissue formulation was 0.5MPa (72.5 psi). It should be noted that the elastic modulus of the breast tissue is the same as the elastic modulus for the implant material, even though these modulii were arrived at using different techniques.

The axial stress-strain relationship for the nonlinear breast tissue material formulation was estimated to be similar to the formulation for all soft tissues. The material formulation used from "The Biomedical Engineering Handbook" [Reference 1], obeys a power law relationship, equation 2.1.1-1.

$$\sigma = K\varepsilon^n \qquad [2.1.1\text{-}1]$$

The two material constants, K and n, were modified using linear regression, to approximate the linear breast tissue material formulation used previously [Reference 3]. The values that are used in the FEA model for K is $3.0*10^6$ and for n is 3.226. This approximation was made due to a lack of breast tissue available for mechanical testing.

2.1.1.2. Shear stress-strain relationship

Both the linear and nonlinear materials formulations for the breast implant assumed that the breast tissue was incompressible. The assumption of incompressibility of the tissue sets Poisson's ratio at a value of 0.45 for linear material models, Poisson's ration for the nonlinear material models was 0.5. A linear material FEA solution cannot invert the stiffness matrix with a Poisson's ratio of 0.5, which is why a Poisson's ratio of 0.45 is typically used in FEA modeling of incompressible materials with linear material formulations. Poisson's ratio is the ratio of shear strain to axial strain. Knowing the axial strain at a location along with Poisson's ratio, allows for the computation of the shear strain at that location. Then knowing the shear strain, Poisson's ratio, and the axial stress-strain relationship, the shear stress can be calculated. This will fully characterize the stress-strain relationships for a material, so by assuming that the breast tissue was incompressible, the shear relationships were specified.

2.1.1.3. Assumption of Homogeneity

As previously stated, the linear and nonlinear breast tissue material formulation assumes that the breast tissue is homogeneous. Without the assumption of the breast tissue being as single material, the FEA analysis could not have been run.

2.1.1.4. Stress Relaxation

No stress relaxation could be modeled, because no mechanical testing could be performed on breast tissue and no previous test data could be located.

2.1.1.5. Preconditioning

Soft tissue preconditioning is the process of cycling from an unloaded state to a loaded state a few times. The loaded state should be only a percentage of the load that is being tested. Preconditioning the tissue allows the tissue to align itself with the load direction, and typically reduces the stiffness of the tissue. Preconditioning is a fact of life when dealing with biotissues. Preconditioning is not considered in this analysis as no data was available nor was actual tissue available for testing.

2.1.1.6. Assumptions

All of the material characteristics for the breast tissue were approximated using soft tissue data. It was also assumed that the temperature dependency for the tissue is insignificant. Tissues formulations that were used were developed based on tests at room temperature, instead of body temperature. This assumption should not significantly affect the FEA results.

2.1.2 General Implant Shell Material Formulation

The implant is manufactured from a silicone rubber, which was testing in an axial load frame to determine the stress-strain relationship for the implant.

2.1.2.1. Axial stress-strain relationship

Linear and nonlinear material formulations were developed from mechanical testing of uniaxial tension specimens. Both the linear and nonlinear implant shell stress-strain formulations were generated from the same data sets, which included 12 axial tests conducted at differing speeds. The linear material analysis showed that the average Young's modulus for the implant material is 0.5 MPa (72.5 psi), the elastic modulus for the implant material was calculated using the axial test data presented in figure 2.1.2.1-1. It should be noted that the elastic modulus for the breast tissue model and implant model are identical, though the elastic modulii were reached using different techniques. The nonlinear material formulation is of a polynomial form, however, the constants were computed birectly by ABAQUS, which accepts the data files as an input for materials that are using the hyperelastic material definition.

Stress and strain are not plotted on figure 2.1.2.1-1 because the data that was inserted into ABAQUS for the nonlinear material formulation requires load vs. displacement data.

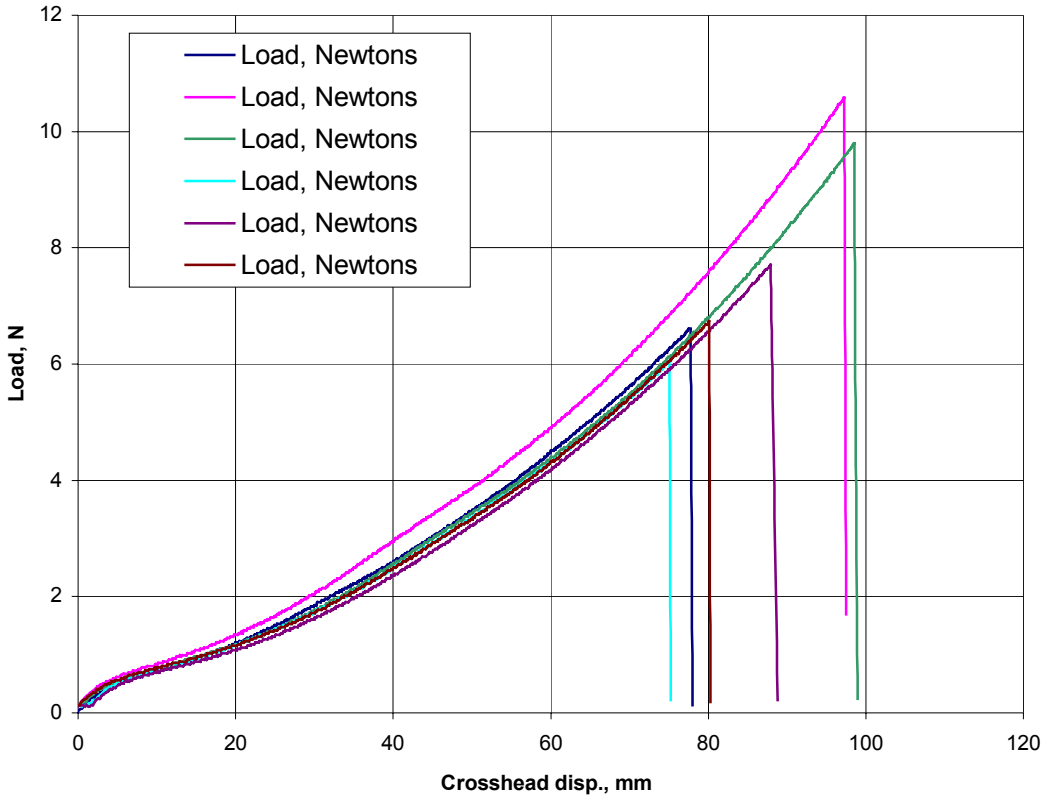

Figure 2.1.2.1-1 Load versus crosshead displacement

2.1.2.2. Shear stress-strain relationship

There was no testing of the implant material for shear characteristics as no torsional specimens could be created. The Poisson's ratio for the implant material was assumed to be 0.5 because most rubber materials are incompressible. As with the tissue material formulation, the assumption of incompressibility fully describes the stress-strain relations for the implant material.

2.1.2.3. Strain Rate

Testing of axial properties was completed at differing speeds, 5mm/min, 10mm/min, 50mm/min, and 500mm/min. Not much quantitative information was gained from this testing. So the assumption of no stress relaxation could be made as the stress-strain curve at differing speeds showed little difference.

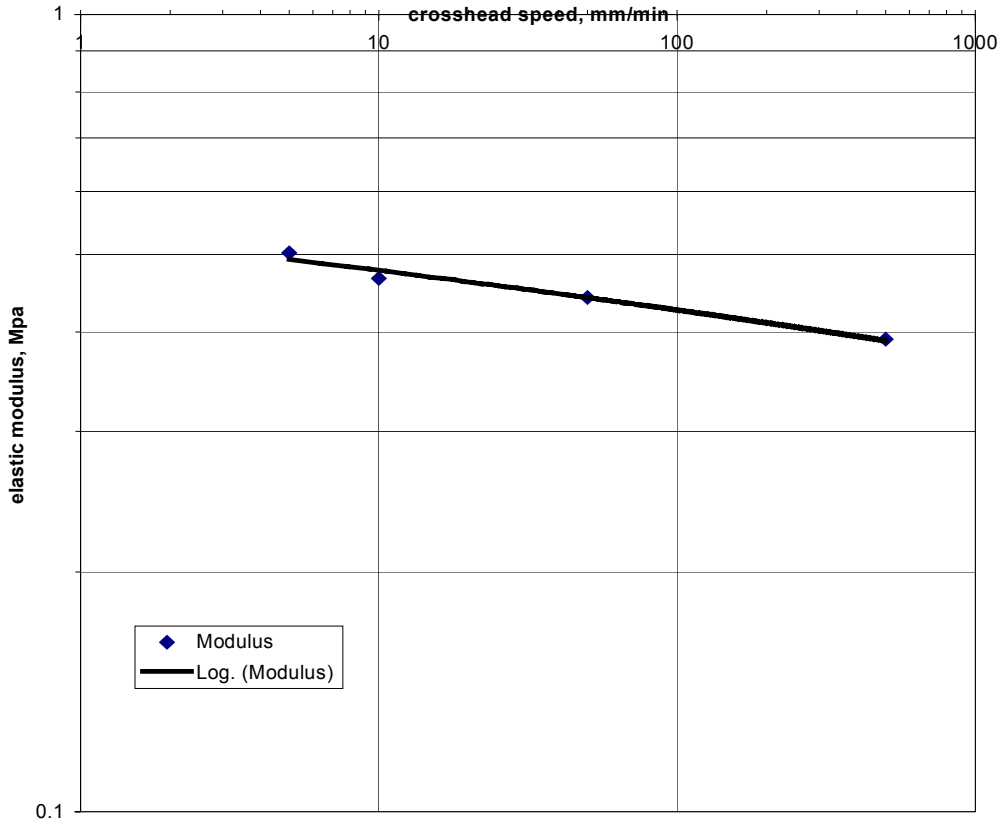

Figure 2.1.2.3-1 Elastic Modulus versus Crosshead speed

2.1.2.4. Mechanical testing

Only the wall of the implant was mechanically evaluated. The patch and valve assembly areas of the implants were not tested because the FEA models do not take into consideration the thickness changes in these areas.

The implant material was tested to determine if there was any dependence on direction for the material characteristics. It was found through random selection of direction and positions on the implants surface. The consistent mechanical properties of the implant independent of direction indicate the material is isotropic. The consistent mechanical properties of the implant independent of the position of the test specimen indicate that the material is homogeneous. Testing different radii and directions relative to the line passing through the center of the implant.

All of the material testing was performed on an Instron uniaxial load tester. The displacement was too large to measure with an extensometer, so the specimen displacement was measured by the crosshead displacement. The load was measured with a 250 N (56.2 lb) load cell. The test specimen was attached to the crosshead and the base of the load tester with pneumatic grips. This is a standard technique for clamping this type of "dog-bone" specimens in a tensile testing machine. Each specimen was cut with a die, yeilding constant and specific dimensions. The specimen dimensions and shape are presented in figure 2.1.2.4-1. The tabs at either end of the specimen were clamped in pneumatic grips so that the radii and the 10.2mm (0.4 inch) test section were exposed while the material tests were conducted.

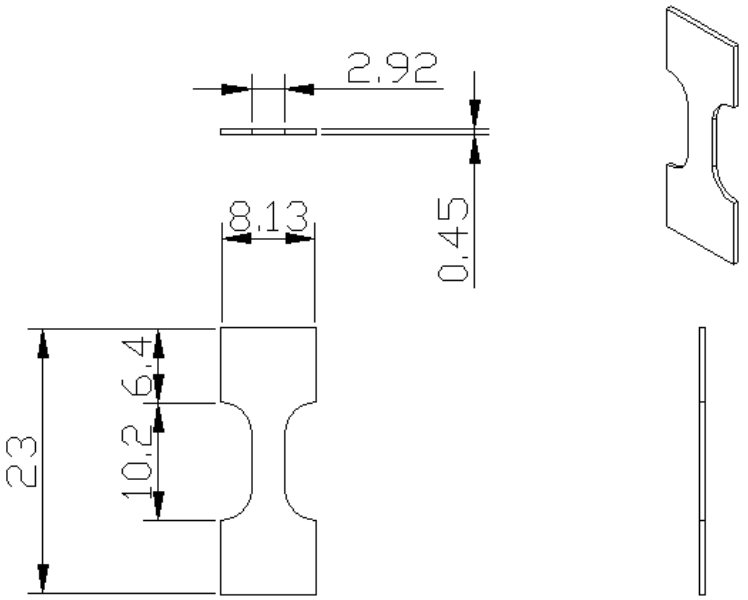

Figure 2.1.2.4-1 Dimensions and shape of the dogbone tension specimen. All dimensions are in mm.

2.1.2.5. Assumptions

The stress-strain relationship for the implant material assumes that there is no change in the mechanical properties due to the small temperature change between room temperature 20ºC (68ºF) and the temperature of the human body 37ºC (98.6ºF). The stress-strain relationships for the implant also assume that no creep will occur and that the stress relaxation of the implant is insignificant.

3. Finite Element Modeling

3.1. General Finite Elements Information

3.1.1 Introduction

Writing Finite Element code is similar to writing C++ code, the code itself is constructed from a series of objects that define the initial geometry, material properties, boundary conditions, component interactions, and external loading. Each FEA model is developed using the same techniques though the information inserted into the FEA code vary with the problem.

3.1.2 Initial Geometry

The models were developed using an axisymmetric geometry definition, meaning that radial symmetry is assumed. The assumption of radial symmetry dictates that the model is two-dimensional yet the resulting stress and strain are determined for a three-dimensional body with no change in the theta or circumferential direction.

The first part of the FEA model that needs to be described is the initial geometry for both the tissue and the implant. The breast tissue geometry is defined as a rectangular block with a parabolic section removed, as shown in figure 3.1.2-1. The initial implant geometry is defined as two-dimensional four degree of freedom axisymmetric beam elements, representing the implant shell along the parabolic curve removed from the tissue geometry. The initial geometries were then meshed using PATRAN. The mammary tissue meshes are present in the tissue area, but the mesh on the implant is to fine to see. The axis of symmetry passes through the center point of the implant, the base

of the tissue represents the ribcage. The right side of the tissue, depending on the boundary condition that is applied to the model, represents either tissue extending into infinity, or a boundary between the tissue block and the exterior of the body, while the top of the tissue block represents the boundary between the breast tissue and the exterior of the body.

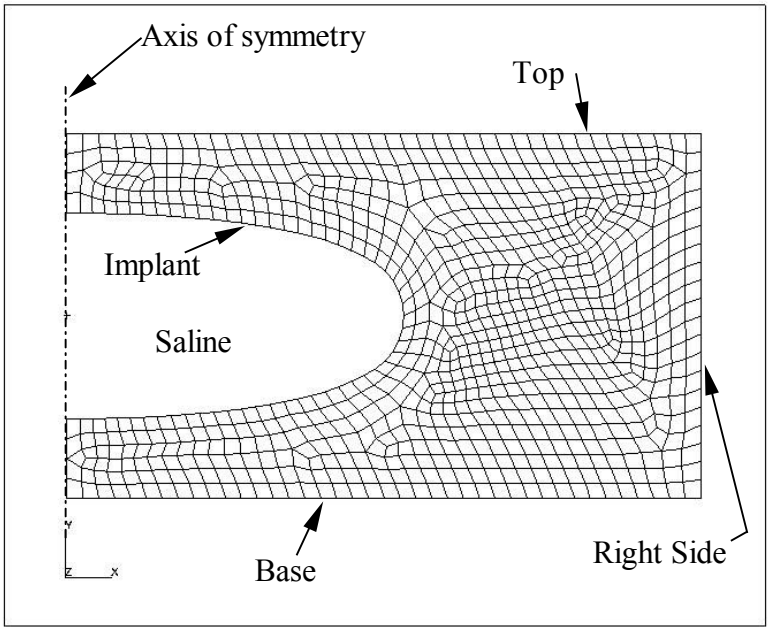

Figure 3.1.2-1: Tissue and implant model, including the mesh, for a non-fold model.

3.1.2.1. Material Models

The second part of the FEA code that is needed is the material property definitions for all of the materials in the FEA model. There are the two solid materials in the FEA and a single fluid material, the two solid materials are the mammary tissue and the implant, the fluid material is the saline that fills the area encased by the implant material. The tissue and the implant use solid material models to define the relationship

between stress and strain. These relationships were detailed in section 2. The saline is modeled exclusively with a hydrostatic formulation of an incompressible fluid. This formulation generates a pressure, driving the implant against the wall when the tissue is externally loaded. Both the tissue and implant material models require the axial and shear mechanical properties. The fluid material formulation only needs the density, as the fluid fills the volume surrounded by the implant. The two different material formulations that were used for the mammary and implant geometries in the FEA model are discussed independently.

There are four material formulations that were defined. The first two material formulations in the FEA model represent the linear and nonlinear material model for the mammary tissue. The second two material formulations that were defined describe the linear and nonlinear implant material models for the silicone membrane model. Details about these models are located in Chapter 2.

Table 3-1 Table showing the Axisymmetric FEA models developed

	Non-Fold models						Fold model
Implant material formulation	Linear	Linear	Non-Linear	Non-Linear	Non-Linear	Non-Linear	Linear
Tissue material formulation	Linear	Linear	Linear	Linear	Non-Linear	Non-Linear	Linear
Right-side displacement constraint	None	Applied	None	Applied	None	Applied	None

3.1.2.2. Boundary Conditions

3.1.2.2.1. Displacement Boundary Conditions

There were four different displacement boundary conditions that were used in the FEA models for the tissue geometry model and only one displacement boundary

condition was placed on the implant geometry model. The first condition defined for the tissue was no prescribed displacement, which allows for total freedom of motion in all directions, this boundary condition was placed on the right side of the model in the models containing no right side boundary condition. The second condition applied to the tissue was a prescribed displacement of zero in all directions, causing the tissue to behave as if it is rigidly attached to a support structure. This boundary condition was placed on the base of the tissue, to simulate the connection of the tissue to the much stiffer ribcage. The third condition placed on the tissue involved zero displacement horizontallly allowing the nodes to slide with no friction vertically this boundary condition was placed on the right side of the tissue in the models containing a right side boundary condition. The fourth condition for the tissue and the only boundary condition placed on the implant was the axisymmetric boundary condition, which defines the axis of revolution for the model overall. The axisymmetric boundary condition allows for motion along the axis of revolution and restrains the associated nodes from retracting from the axis of revolution.

Each of the boundary conditions is reiterated in each of the specific model descriptions.

3.1.2.2.2. Contact Boundary Conditions

The primary interaction between the different components in the FEA model is contact. The contact either occurs between two different model components, like between the implant and tissue, or self contact. All contact models require inputs defining the contact model to be used between the surfaces contacting each another. The contact definition values include the nodes that create the contact surfaces, the static and kinetic coefficients of friction, the separation properties for the contact, defining the deformation

characteristics of the master and slave elements. The master element in the contact model can be defined as either rigid with respect to the contact or deformable with respect to the contact. If the master element is defined as rigid all of the deformation in the contact will occur in the slave element, if the master element is defined as deformable then deformation will occur in both the master and slave element. Some of the contact properties were consistent in all of the contact definitions, while other parameters like the separation properties varied between the contact definitions.

There was one contact surface set defined in each of the FEA models. The first contact surface in the set was the implant. The second contact surface in the set contained the nodes of the tissue contacting the implant. This contact surface set was then modeled into a contact pair, with one contact surface being defined as the master surface, the other surface being the slave. Both surfaces in the contact pair were defined as deformable surfaces. The friction and separation properties were varied in each FEA model to determine the best definition while all of the other properties were held constant. Each contact property is described below to show the possible interactions that could be modeled between the implant and the tissue. An ABAQUS feature automatically defines self-contact for all structures that are modeled, which means that the structures can contact themselves, generating the correct contact forces according to the contact definition.

The coefficient of friction in the contact model determines whether two surfaces while in contact with each other can slip relative to one another. ABAQUS has two different formulations depending on the contact definition that is desired. The first input defines the contact with a no slip friction model, which translates to having an infinite

coefficient of friction allowing no slip between the surfaces regardless of the normal or shear forces. An infinite friction coefficient defines the no slip condition. The second friction definition requires a coefficient of friction to be commanded by the user. The coefficient of friction that can be inserted into ABAQUS for this model may vary from 0 to near infinity. Defining a coefficient of friction allows for surface interactions along the tangential direction of the surfaces based on the normal contact force. If the coefficient of friction is zero, then the surfaces have no resistance to slip. If the coefficient of friction is greater than zero, then the amount of tangential force resisting slippage is proportional to the normal force multiplied with the coefficient of friction.

Four separation models define the separation properties between surfaces contact. The first model allowing no separation is most often used in analysis, defining a perfect bond between the two surfaces. The second model defines hard separation, such that when the normal contact pressure is equal to or below zero the two surfaces are not in contact with each other, this means that either the surfaces are in contact or they are not in contact. The third separation model is the modified hard separation model, where the normal contact pressure that determines separation is defined as a user input, the contact pressure input may be any value. The second and third models only apply the contact model if the separation pressure requirement is met otherwise there is no contact. The final separation model is the exponential separation model that allows for a user defined gradual separation curve. The exponential separation model allows for a gradual reduction in the contact model application based on the separation curve. The hard separation and exponential separation models were used in this project, though all of the models were tested in the implant-tissue models to determine which worked the best.

3.1.2.2.3. Loading Boundary Conditions

There are two external loading objects that were used in this projects FEA models. The first object defines a distributed load applied to a surface. With the implant-tissue models the distributed load was applied across the top of the tissue. The second loading object used is a fluid pressure. The fluid pressure in all of the models except the fold model was zero, indicating that the fluid was present but no applying any pressure on the implant initially. After the solution has been run the internal fluid pressure in the implants rises.

3.1.2.3. Solution Process

All of the FEA solutions use a nonlinear solution step procedure. Through ramping up the load and using a step solution technique, the solution converges when either large displacements or nonlinear initial geometries are present in the problem. The FEA models for this project include both, large displacements because of the low stiffness, due to thin implant walls, and nonlinear geometry of the implant. This solution technique iterates through the solution space in steps, slowly ramping the loads up after each converged iteration step. If the iteration step does not converge then the step length and therefore the load is reduced and the iteration is rerun. This nonlinear solution step procedure is part of ABAQUS and is used when the user defines that the problem is nonlinear.

3.1.2.4. State of Stress

Understanding the state of stress on the implant wall is crucial to understanding the results generated in the FEA analysis. Three stresses were computed for the tissue in

the analysis. The axial stress in the x and y direction and the shear stress in the x-y plane were computed. The stresses in the implant are computed along the element, and then decomposed into the x and y direction by ABAQUS. Because of the ABAQUS element formulation the computed stresses in the implant shell are the magnitudes of the stresses along the axis and do not identify the compressive or tensile nature of the implant stress. In order to determine the compressive or tensile nature of the stress in the implant, the contact model between the tissue and the implant is used to infer the nature of the stress. The contact model between the implant and the tissue defines that there is no slip between the implant and the tissue, this means that if the local tissue stresses are compressive then the stress in the implant would also be compressive, while tensile tissue stresses would mean that the implant stress was tensile.

3.1.2.5. General Conclusions

The most significant data obtained by the FEA analysis is that of the stresses and displacements in both the tissue and the implant under given external loads. The displacements were computed in both the x and y directions. The axial and shear stresses for both the implant and the tissue were also determined using the same FEA models. The Von Mises stress was then computed based on the axial and shear stresses.

$$\sigma_{\text{Von Mises}} = \frac{1}{\sqrt{2}}\sqrt{(\sigma_x - \sigma_y)^2 + (\sigma_y - \sigma_z)^2 + (\sigma_z - \sigma_x)^2 + 6(\tau_{xy}^2 + \tau_{yz}^2 + \tau_{xz}^2)} \qquad \text{Equation 3.1.2.4-1}$$

The various stresses that were computed and presented are the Von Mises, axial in the x and y directions, shear in the x-y plane, and the principal stresses. Von Mises stress is an energy average stress, which is positive definite and is typically used in failure predictions. Because this stress is always positive it cannot indicate compressive loading.

The axisymmetric FEA models are not computationally capable of predicting buckling of the implant because it would be a local phenomenon, and at initiation the buckled area would not be symmetrical. This means that the only way to identify local buckling would be to generate a three-dimensional FEA model defining the boundaries between the breast tissue and the implant such that the possibility for buckling is included in the model definition. If the local stresses in the implant are compressive then there is a possibility that the membrane could buckle which could lead to fold flaw formulation. Information that has been given from Mentor Corporation is that there have been implant failures, which included a crease; this crease could be explained by local buckling of the implant.

As with all computational analyses only the objects specifically defined in the computer model are present in the analysis. These models are only approximations, and that there are many assumptions that are present throughout. The specific model inputs are discussed for each of the five different models, the assumptions made are pointed out, and the justification for each assumption is detailed.

3.2. Implant Models and Results

3.2.1 Linear implant and tissue material models, with non-linear geometry, and no right side displacement constraint

3.2.1.1. Specific Initial Geometry

The initial geometry for the tissue is shown in figure 3.1.2-1. The implant lies along the inside of the cavity, with the fluid control node defined at the center of the cavity. The tissue block is 101.6mm (4 inches) long in the x direction, and 58.42mm (2.3 inches) thick in the y direction. The cavity is modeled as a parabola. The shape and dimensions for this model were taken directly from the previous research [Reference 3].

3.2.1.2. Specific Material Models

Both the tissue and implant material formulations in this model are linear elastic. The specific material model information for the tissue and implant is defined according to the linear elastic material definitions in section 2.

3.2.1.3. Specific Boundary Conditions

The base, or bottom points of the tissue, were given fixed zero displacements in both the x and y directions, to simulate the rigid attachment of the tissue on the ribcage. The top and right side of the tissue was left unconstrained to motion; the top was subjected to an applied distributed load applied in the vertical direction. The left sides of the tissue, as well as the leftmost points on the implant have the axisymmetric boundary condition; restricting these implant and tissue nodes from moving in the x direction while allowing unrestrained motion in the y direction. The bottom right and bottom left points

are both fixed. The internal fluid pressure in the center of the implant was set a 0 kPa (0 psi), simulating an initial case were the implant was perfectly fit into the tissue cavity and the implant was filled completely without pressure loading the implant. While the fluid pressure is not necessarily zero at implantation, the implant pressure was assumed to be zero to simplify the model.

3.2.1.4. Specific Component Interactions

The only interactions between the model components are between at the fluid-implant boundary and the implant-tissue boundary. The interaction between the fluid and the implant was defined by meshing the two material objects identically, which was required for the analysis to compute a solution. There is no ABAQUS definition in the input files that defines the interaction between the implant and tissue, however, the same nodal points were defined for both of these components. Defining the implant and fluid in this way binds the two surfaces between implant and tissue together, generating a no separation and no slip interaction. The second interaction, between implant and tissue, is defined by modeling the contact between these two surfaces. The tissue is defined as the master surface while the implant is defined as the slave. The interactions between the tissue and implant surfaces were defined with the no slip and no separation conditions. Rigidly attaching the implant and tissue together.

3.2.1.5. Specific External Loading

The external load inputted to the model was a single distributed load across the top of the tissue model. The pressure applied by the load was 116.37 kPa (16.88 psi) down. This load was selected because it is the highest load that would converge to a

solution, yielding the highest stresses. This linear elastic FEA model was also run for 10 kPa (1.45 psi) and 15 kPa (2.18 psi) both of which are more realistic loads that might be applied to the tissue. It was found that the stress and displacement fields that resulted from these three loading conditions were an order of magnitude different, though the maximum and minimum displacements and stresses occurred in the same areas.

The maximum stress in each of the three runs of this model was caused by the fixed boundary condition on displacement applied to the bottom of the tissue and the lack of displacement constraint on the right side of the tissue. This maximum stress, occurring at the right side of the base, is an artifact of the model, and not truly representative of the case in vivo (in human body). This artifact was caused by constraining this point to zero displacement without constraining the other nodes making up the right side of the tissue model.

3.2.1.6. Results

Results are shown in figure 3.2.1.6-1 through 3.2.1.6-7 for an applied tissue pressure of 116.37 kPa. Most of the stresses around the implant shell are tensile. Analysis of the tissue stresses, figures 3.2.1.6-4 and 3.2.1.6-7, show that the boundary between the tissue and the implant is compressive in the x and y directions everywhere. Because the implant is connected to the tissue though a no-slip condition, the state of stress in the implant is also compressive in both the x and y directions. The magnitudes of the implant stresses are presented in figures 3.2.1.6–3 and 3.2.1.6-6. The compressive stresses in the implant at the far right are very significant. The main complication with the compressive stresses in the implant is that the implant has a very small bending rigidity. It is believed that the compressive stresses in the implant, coupled with the low

resistance to bending could lead to buckling even though the implant was perfectly sized for the pocket. The Von Mises stress at the tip of the implant, presented in figure 3.2.1.6-1, is between 107 kPa (15.52 psi) and 98.1 kPa (14.23 psi), with a maximum compressive stress in the x direction, figure 3.2.1.6-3, of –78 kPa (-11.31 psi). The largest and smallest Von Mises stresses in this model are 159 kPa (23.06 psi) and 28.4 kPa (4.12 psi), respectively. The axisymmetric model is not capable of predicting whether buckling will occur because buckling will not occur at the same radial location. To accurately determine the buckling characteristics at the right side of the implant, a three-dimensional implant would need to be developed and buckling analysis would need to be preformed. The tissue Von Mises stresses, presented in figure 3.2.1.6-2. Figures 3.2.1.6-4 and 3.2.1.6-7, show the tissue stresses. These stresses were used to determine the implant stress directionality, as discussed in chapter 3.1.2.4.

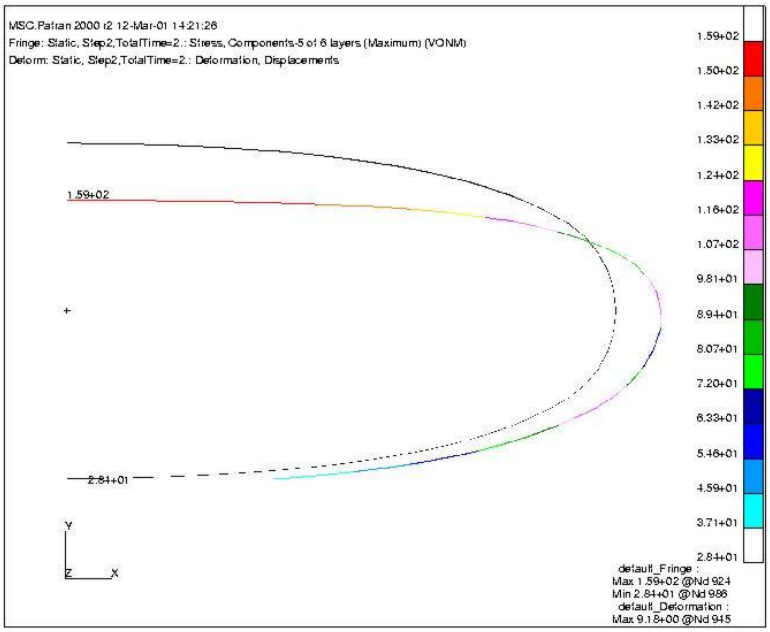

Figure 3.2.1.6-1: Von Mises stresses in the implant

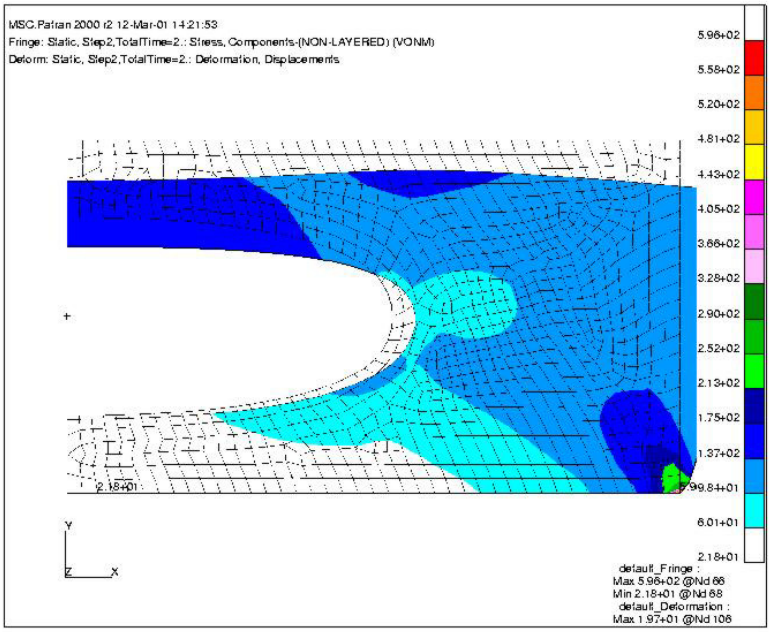

Figure 3.2.1.6-2: Von Mises stresses in the tissue

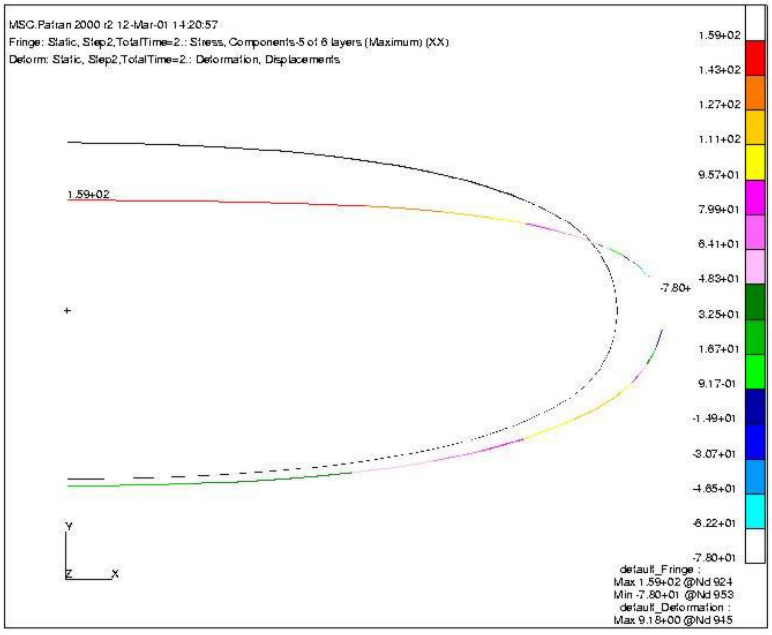

Figure 3.2.1.6-3: Stress in the implant along the x direction

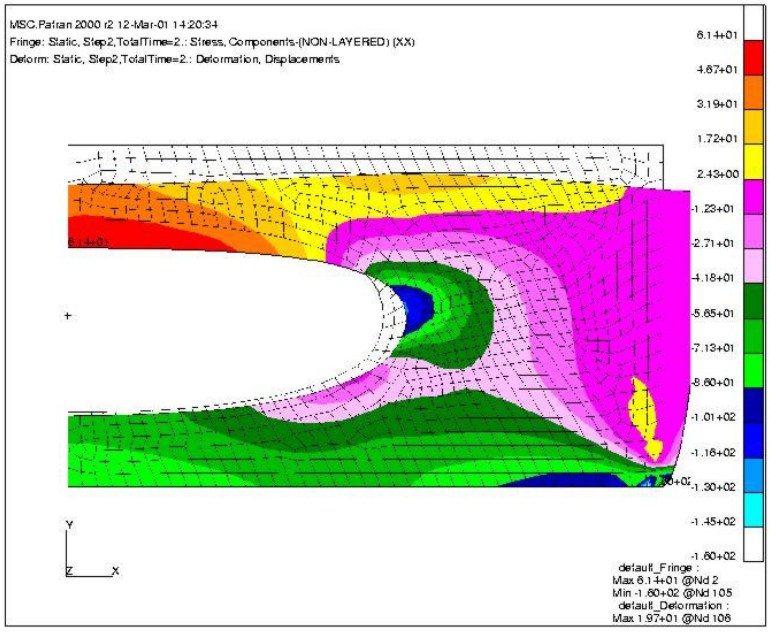

Figure 3.2.1.6-4: Stress in the tissue along the x direction

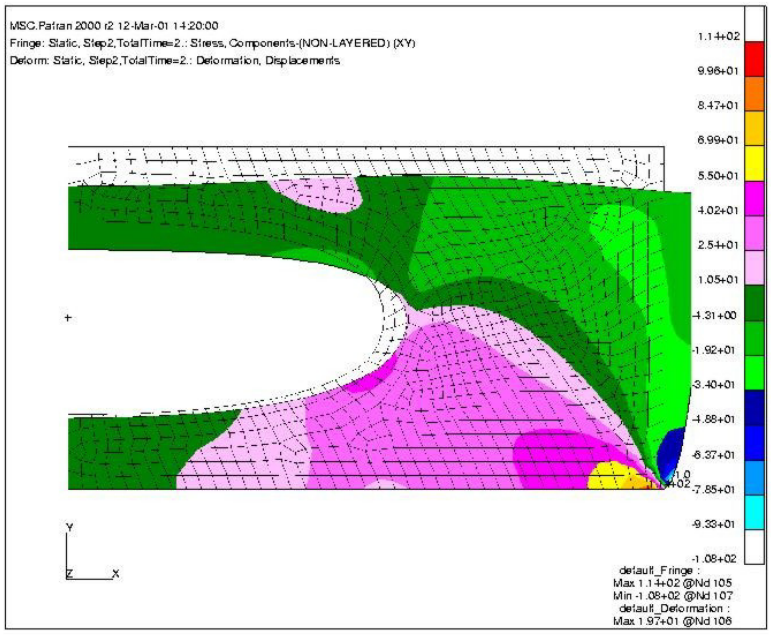

Figure 3.2.1.6-5: Shear stress in the tissue in the x-y plane

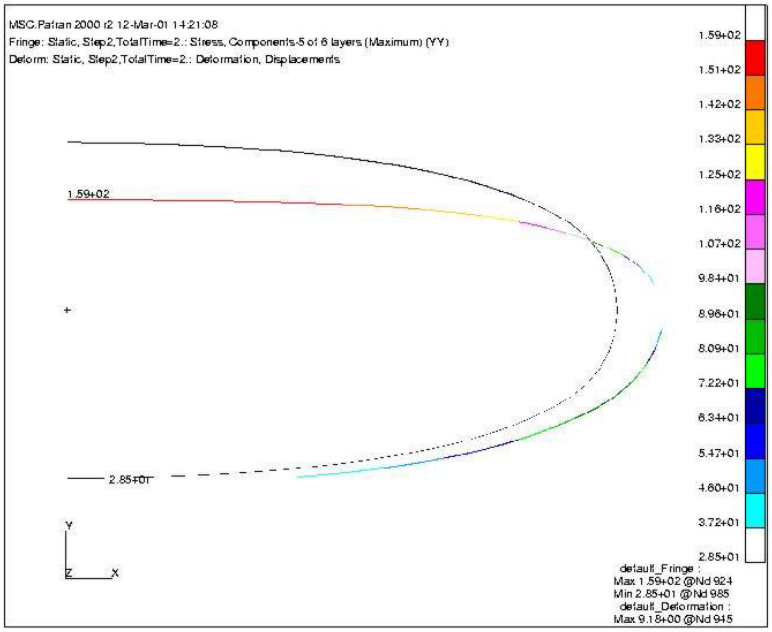

Figure 3.2.1.6-6: Stress in the implant along the y direction

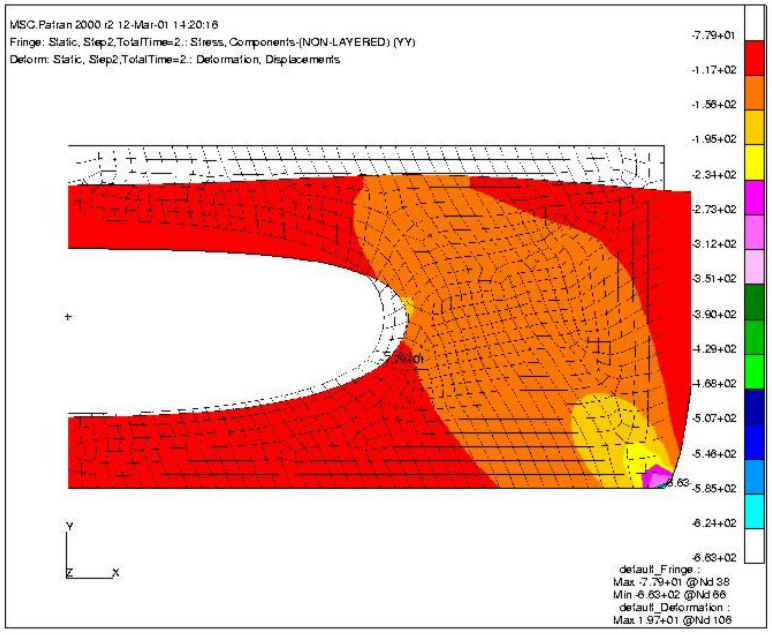

Figure 3.2.1.6-7: Stress in the tissue along the y direction

3.2.2 Linear implant and tissue material models, with non-linear geometry and with a right side displacement constraint

3.2.2.1. Specific Initial Geometry

The initial geometry of this model is identical to the geometry of model 3.1. The tissue was a block of 101.6 mm by 58.42 mm (4 in by 2.3 in). The implant was again parabolic; since the initial geometry of this model is the same as model 3.1, figure 3.2.2.6-1 represents to initial geometry.

3.2.2.2. Specific Material Models

Both the linear implant and linear tissue material models were applied to the respective geometries. The modulus of elasticity and Poisson's ratio for both the tissue and the implant are defined in the model according to the information presented in Section 2.

3.2.2.3. Specific Boundary Conditions

The prescribed displacement in both the x and y directions on the bottom of the tissue block was 0. The right side of the tissue block had a displacement boundary condition in the x direction of 0, however the tissue block was allowed to deform freely in the y direction. This set of boundary conditions simulates a far field where tissue resists motion in the x direction and allowing the tissue to move vertically. The top of the tissue block had no displacement conditions placed on it so the top tissue surface is free to move in any direction. The left side of the tissue and the two left most nodes of the

implant had the axisymmetric boundary condition assigned to them. This allows for motion in the y direction, but not in x.

3.2.2.4. Specific Component Interactions

There are only two component interactions in this model. The first interaction was the contact between the implant and the tissue while the second interaction was between the fluid and the implant. In the first interaction definition the implant was defined as the slave surface and the tissue was defined as the master surface. The friction between the implant and the tissue was defined to be rough meaning no slip and no separation allowable for the implant from the tissue. The interaction between the implant and fluid was not explicitly defined; through the nodal definition there is no separation and no slip. The fluid and implant are always in contact with each other; there is no master or slave surface in the implant-fluid interaction because the implant and fluid do not have an explicit interaction definition.

3.2.2.5. Specific External Loading

The distributed load applied to this model in the down direction was 249.69 kPa (36.22 psi). The difference between this model and model 3.1 is that this model does not have the large tissue displacement in the x direction at the right of the tissue block. Constraining the motion on the right side of the implant the FEA model gives a more accurate representation of the actual implant-tissue system.

3.2.2.6. Results

The stress in the x and y direction at the tip of the implant are –33 kPa (-4.79 psi) and .38 kPa (0.055 psi), respectively. The stresses in the implant are again compressive,

as indicated by the state of stress in the tissue. The compressive stresses in the implant indicate that buckling of the implant may occur. These stress plots are presented in figures 3.2.2.6-1 through 3.2.2.6-7. The maximum and minimum implant Von Mises stresses are 36kPa (5.22 psi) and 15.1 kPa (2.19 psi), respectively. The maximum implant Von Mises stress occurred at the implant tip, so the 33 kPa (4.79 psi) compressive stress is amongst the largest stress in the entire solution. The Von Mises stress of the tissue is displayed in figure 3.2.2.6-2.

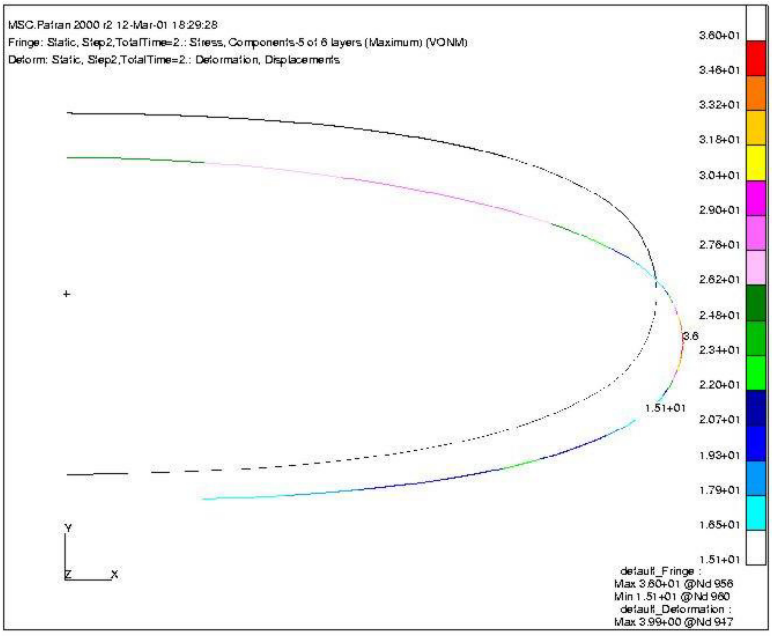

Figure 3.2.2.6-1: Von Mises Stress in the implant

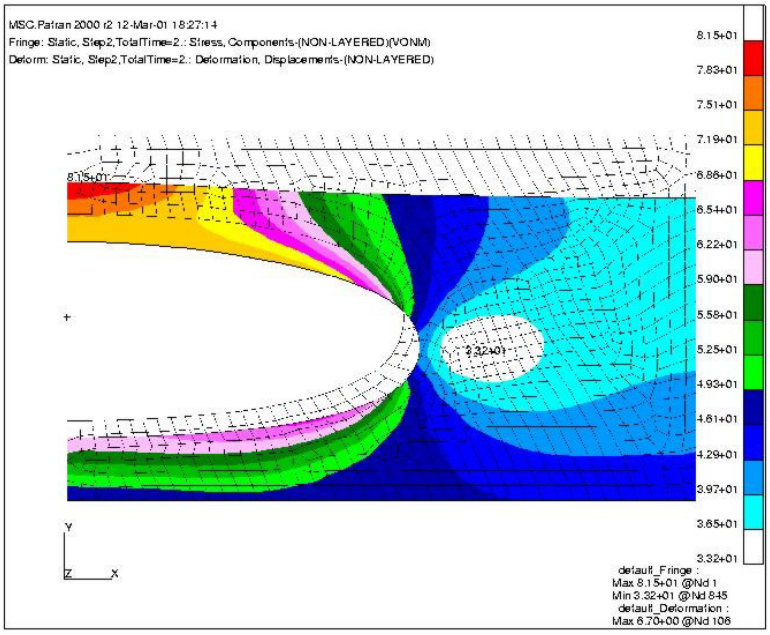

Figure 3.2.2.6-2: Von Mises stress in the tissue

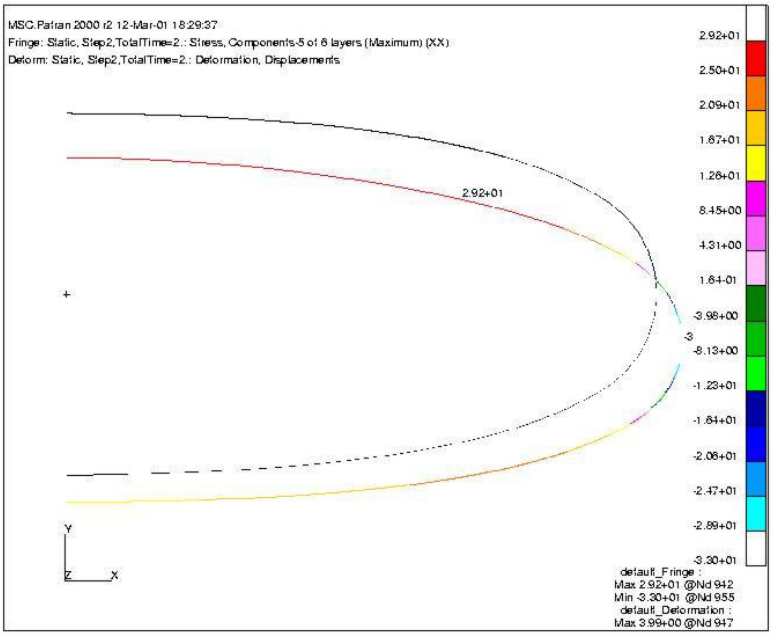

Figure 3.2.2.6-3: Stress in the implant along the x direction

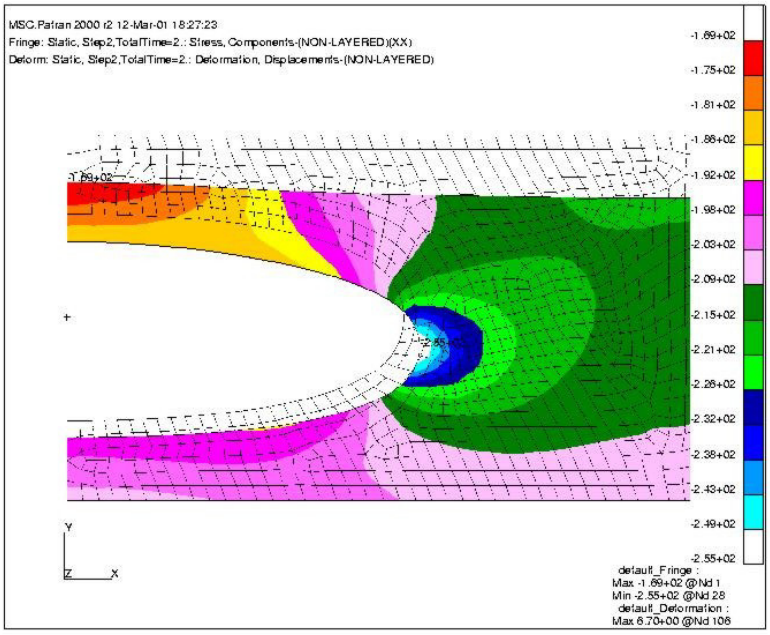

Figure 3.2.2.6-4: Stress in the tissue along the x direction

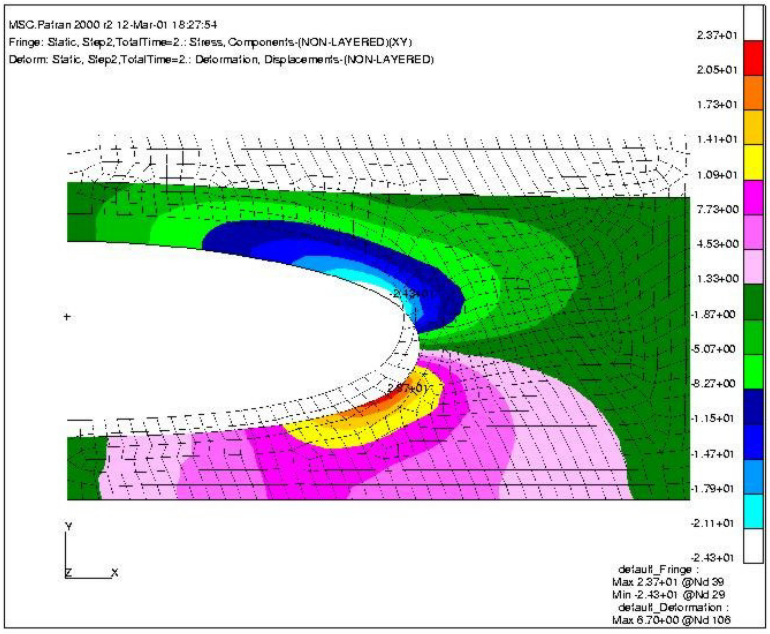

Figure 3.2.2.6-5: Shear stress in the tissue in the x-y plane

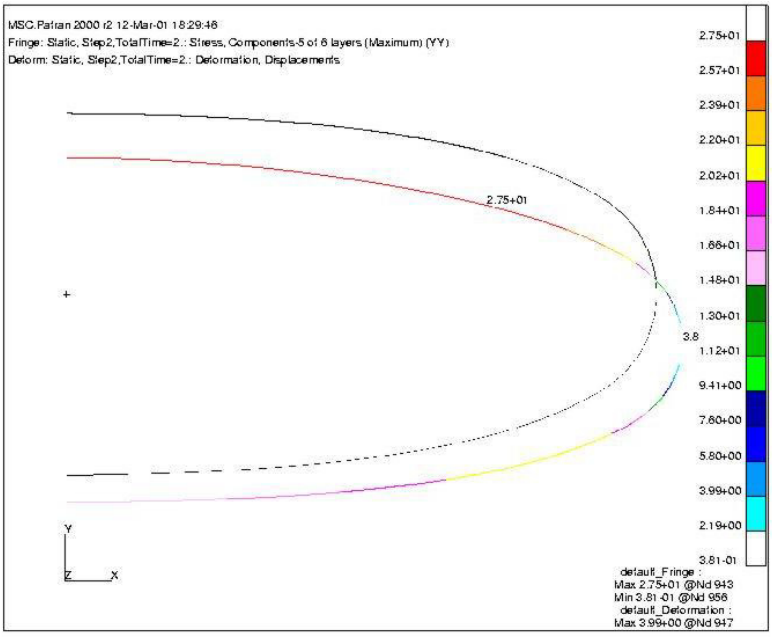

Figure 3.2.2.6-6: Stress in the implant along the y direction

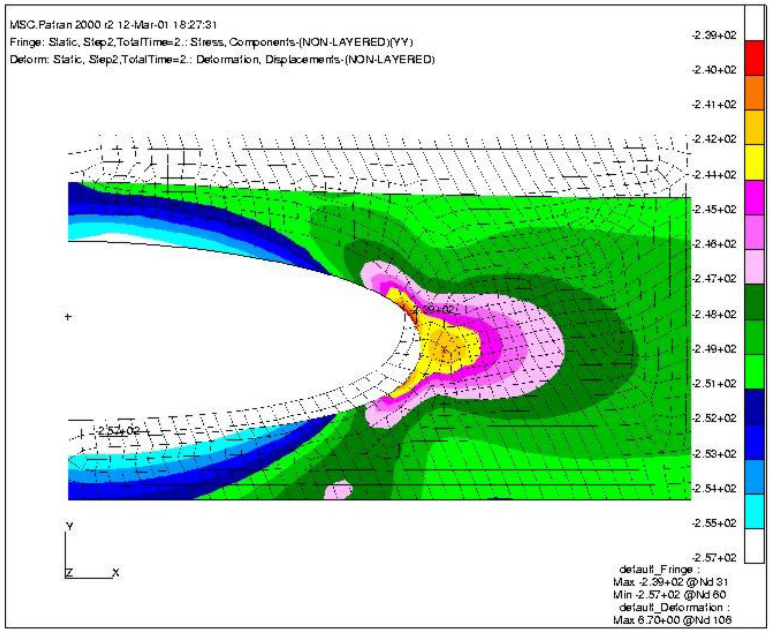

Figure 3.2.2.6-7: Stress in the tissue along the y direction

3.2.3 Linear tissue and implant material models, with nonlinear geometry and inclusion of a fold

3.2.3.1. Specific Initial Geometry

The initial geometry of this tissue is identical to the two previous models; the initial implant geometry is quite different. This model was used to investigate the stress increase that is caused when a fold is forced to develop in an axisymmetric implant-tissue model. For this model the implant pulled away from the tissue wall at the right edge of the cavity so that the implant is actually larger than the cavity forcing a fold to develop. The implant in this model is larger than the cavity that it fits into, so a fold must develop when the cavity is pressurized. The initial implant and tissue geometry is presented in figure 3.2.3.1-1, along with the mesh that was used for solving this problem.

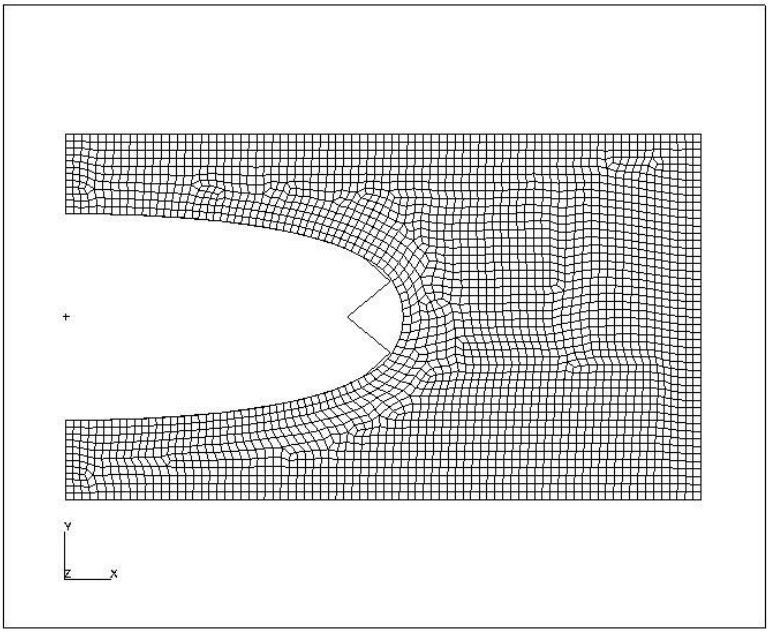

Figure 3.2.3.1-1: Plot showing both the tissue and the implant, for the fold model

3.2.3.2. Specific Material Models

The same linear tissue formulation and linear implant formulation is used in this model, see Section 2 for more information about these material formulations.

3.2.3.3. Specific Boundary Conditions

There are the same displacement boundary conditions applied to this model as there were for the linear implant and tissue model with no right side boundary condition. These include a fixed 0 displacement in the x and y directions for the bottom of the tissue, no right side or top displacement boundary condition for the tissue, and an axisymmetric displacement boundary condition for the left side of the tissue and the left most points on the implant. The internal fluid pressure condition for this model sets the implant pressure to 1.0 kPa (0.145 psi). This increased pressure is required to load the implant fold, as no external loading of the tissue was used.

3.2.3.4. Specific Component Interactions

There were three contact interaction models between the implant and the tissue; one of these interactions was defined differently than the previous models. The contact model included no separation, and a slip tolerance in the slip direction of 0.02. The slip tolerance condition is the ratio of allowable elastic slip to the characteristic contact surface dimension. This allows for some limited sliding in the slip direction, but not much as the surface characteristic contact dimension is very small.

The second enforced interaction was a condition of self-contact on the implant, which treated the implant as both the master and the slave in the contact interaction. This allowed for the implant to slide on itself without passing through itself. This condition is

applied by ABAQUS for all materials, and the definition was not changed for this analysis.

The third interaction is not defined in the usual way, by tying the implant nodes to the fluid nodes together these two components are forced to remain together. There is no slip on the boundary; there is also no separation, between the implant and the fluid.

3.2.3.5. Specific External Loading

There was no external loading in this model. The lack of external loading produces the bulge in the tissue for the solutions to this model. The internal fluid pressure is the only applied load; this was done so that the stress increase caused by the fold in the implant could be compared, between the unloaded implant and the folded implant. An unfolded implant, with no external loading, would not be internally stressed.

3.2.3.6. Results

The Von Mises stresses in the implant at the tip of the fold are 78.7 kPa (11.41 psi), which is the largest Von Mises stress in the implant; the minimum Von Mises stress in the implant was 3.89 kPa (0.56 psi). The stresses in the center of the fold are 20 times higher than the lowest stresses in the implant. The majority of the Von Mises stresses in the implant away from the fold are approximately 23 kPa (3.34 psi), which is three times less than the stress at the tip of the fold. This stress information is displayed in figure 3.2.3.6-1. The tissue after the fold is developed also has some internal stresses, and these internal Von Mises stresses are presented in figure 3.2.3.6-2. The implant and tissue stresses in the x and y directions were also computed, and these stresses are displayed in figures 3.2.3.6-3 through 3.2.3.6-7.

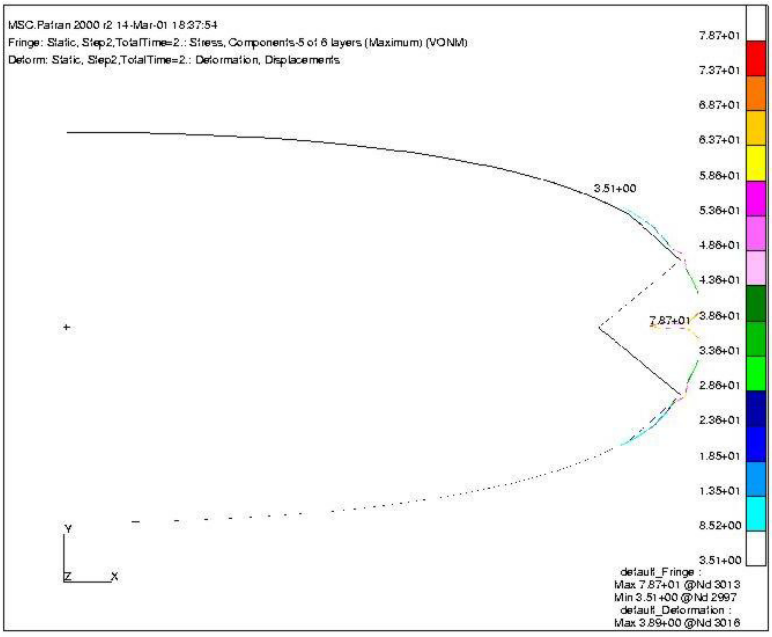

Figure 3.2.3.6-1: Von Mises stresses in the implant

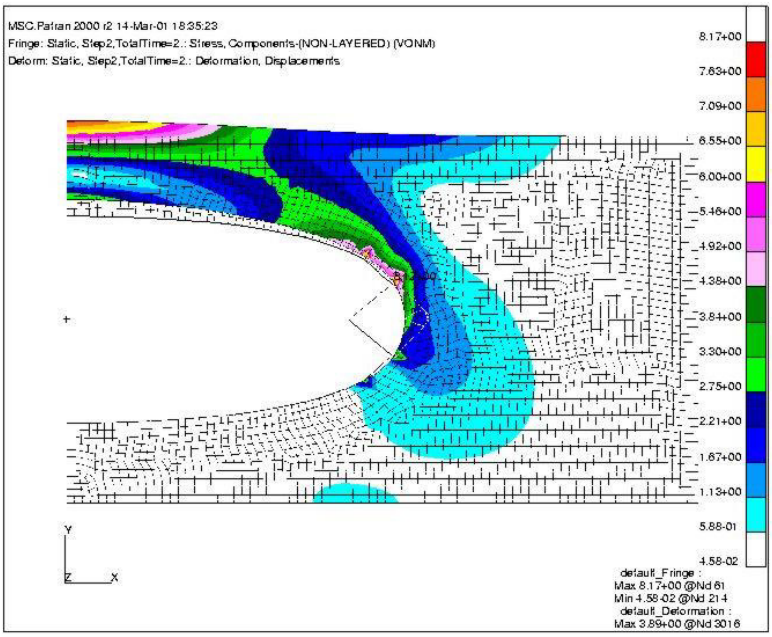

Figure 3.2.3.6-2: Von Mises stresses in the tissue

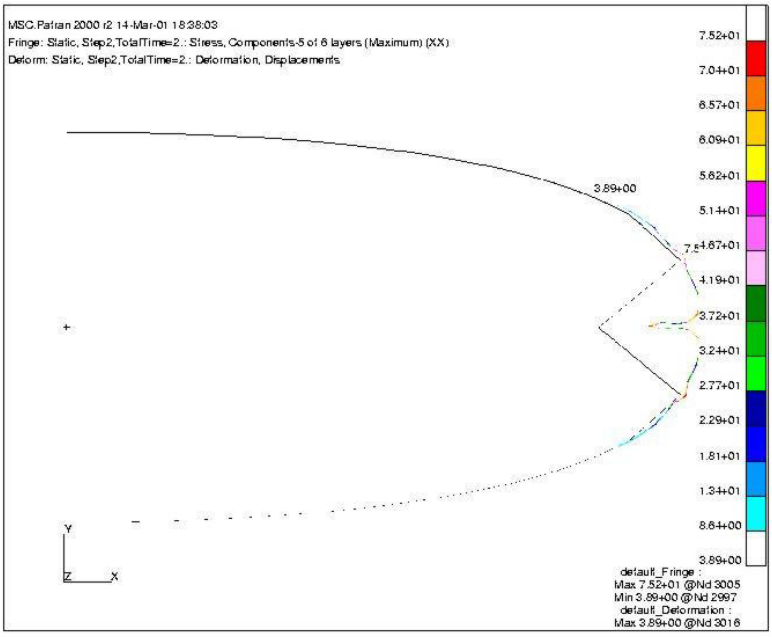

Figure 3.2.3.6-3: Stress in the implant along the x direction

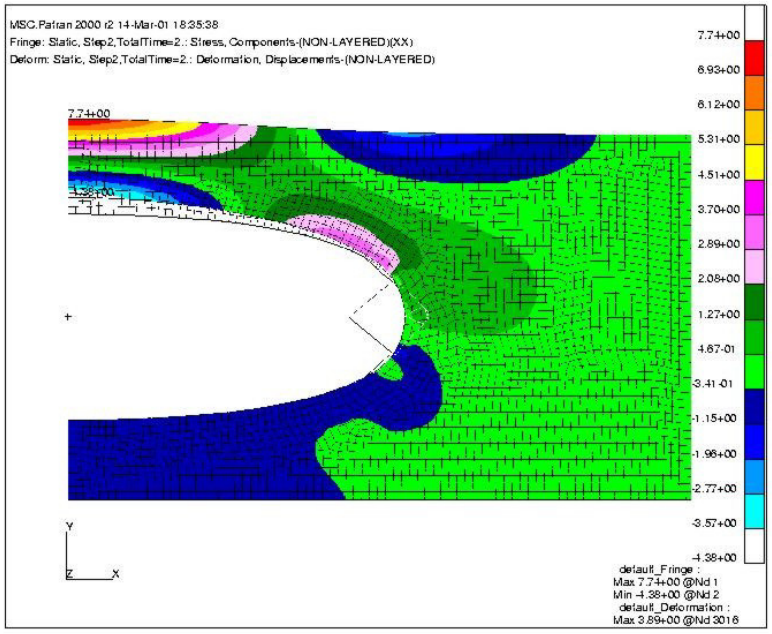

Figure 3.2.3.6-4: Stress in the tissue along the x direction

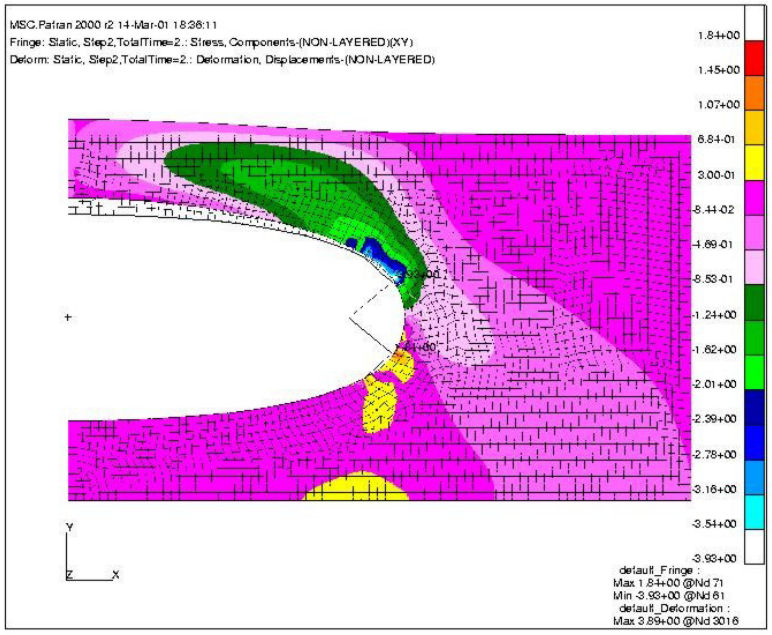

Figure 3.2.3.6-5: Shear stress in the tissue in the x-y plane

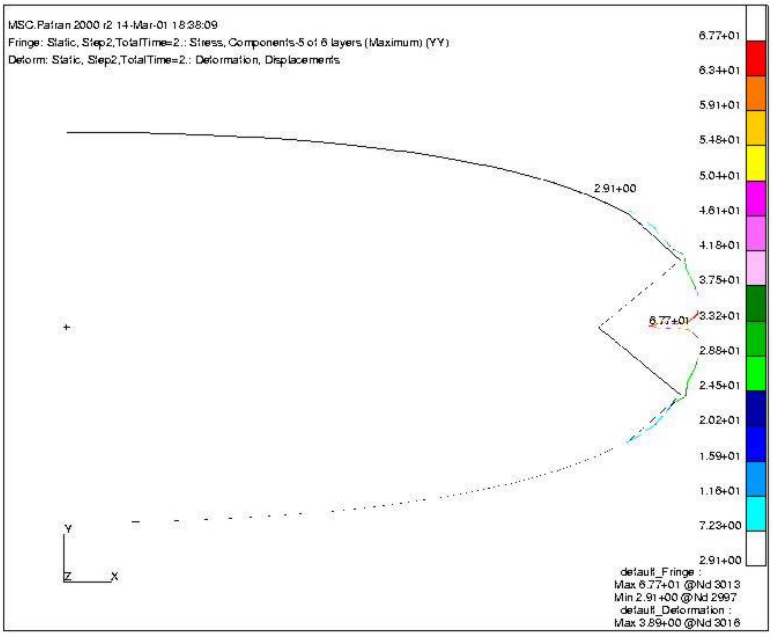

Figure 3.2.3.6-6: Stresses in the implant along y direction

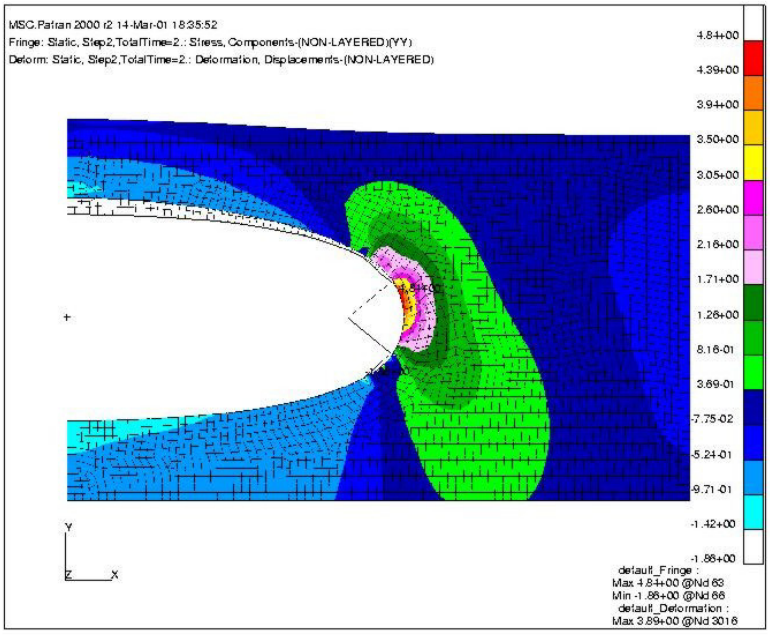

Figure 3.2.3.6-7: Stress in the tissue along the y direction

3.2.4 Nonlinear implant and tissue material models, with nonlinear geometry and no right side displacement constraint

3.2.4.1. Specific Initial Geometry

The initial geometry of the tissue and implant is identical to models 3.1 and 3.2. The figure of the initial geometry and the tissue mesh is figure 3.1.2-1.

3.2.4.2. Specific Material Models

The material formulations in this model are nonlinear for both the tissue and the implant. The nonlinear tissue material formulation was developed as described in Section 2. The implant formulation was defined by ABAQUS using the stress-strain data from a 50 mm/min axial tension test. The ABAQUS nonlinear material formulations allow for Poisson's ratio to be set at 0.5 as detailed in Section 2. The nonlinear tissue material needs further investigation because ABAQUS identifies that the nonlinear tissue model to be unstable, though the ABAQUS documentation does not give any information about the type of instability in the formulation. Because no material tests could be performed to determine what might is incorrect in the material model, there is no way to correct the unstable nature of the tissue model without biaxial stress-strain data for the tissue. The biaxial stress-strain data will also allow for more accurate FEA results for the tissue stresses.

3.2.4.3. Specific Boundary Conditions

The points along the base were constrained in both the x and y direction with zero displacements, the motion of the right side was not constrained, because of the low forces

applied in this model. The top was not constrained from motion in any direction direction, though the top of the tissue was loaded with a vertical distributed load. The left side of the implant had an axisymmetric boundary condition, which means that the side could be displaced vertically but not horizontally. The internal fluid pressure was set at 0 kPa (0 psi).

3.2.4.4. Specific Component Interactions

The interactions in this model are between the implant and the tissue, and the implant and the fluid. Setting the finite element nodes at the same locations generated the interaction between the implant and the fluid. The interaction between the implant and the tissue is generated through a contact definition. In the tissue-implant interaction the tissue was defined as the master surface with the implant defined as the slave. The interaction between the tissue and the implant is defined with the no slip and no separation condition, which means that the tissue and implant had an infinite friction between them, and the implant could not separate from the tissue.

3.2.4.5. Specific External Loading

The only external load was applied to the top of the tissue, and consisted of a single distributed load, in the vertical direction. The applied load was -24.0195 kPa (-3.48 psi) down. This is the only load in the entire model, and it indicates the maximum load that yielded a solution. The model was then run for 10 kPa (1.45 psi) and 15 kPa (2.18 psi), which are more realistic for loading in the human body.

3.2.4.6. Results

The maximum Von Mises stress in the implant occurred at the axisymmetric boundary condition, while the maximum stress in the x-direction, 53.9 kPa (7.81 psi) occurred on the right side edge of the implant. The maximum stress in the implant y-direction has a magnitude of -10.9 kPa (1.58 psi) at the same location as the maximum x-direction stress in the implant, which is an artifact of the model. The maximum stresses in the tissue occur at the far right side of the tissue block, were the tissue is constrained as the bottom, this should not be the case for a tissue model that was constrained in the x direction. The fact that the maximum stress occurred in the lower right corner of the tissue block is an artifact generated by the formulation of the boundary conditions, identical to model 3.2.1.

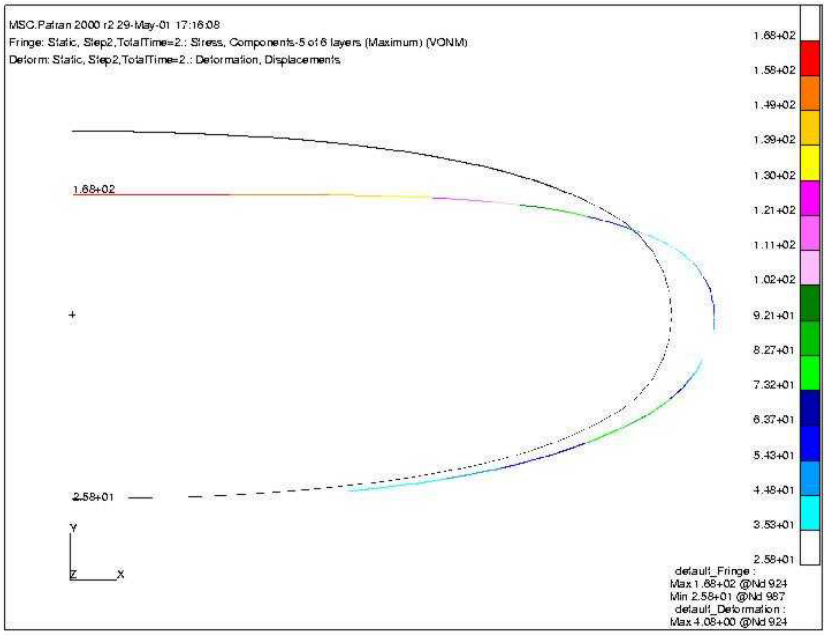

Figure 3.2.4.6-1 Von Mises stresses in the implant

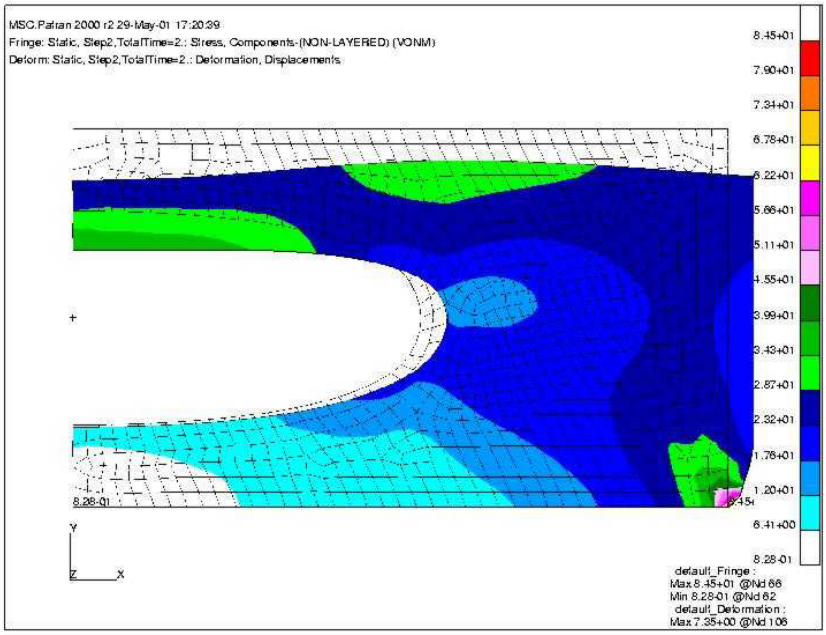

Figure 3.2.4.6-2 Von Mises stresses in the tissue

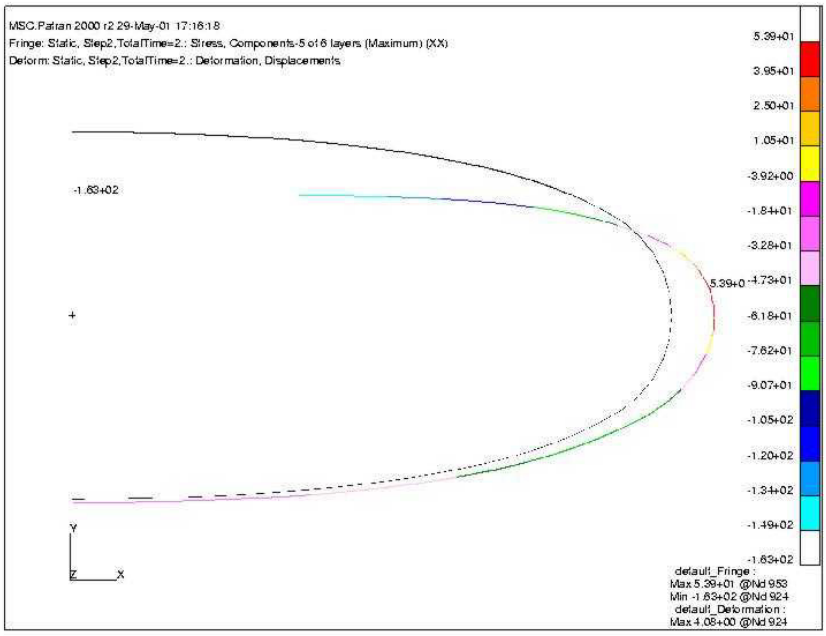

Figure 3.2.4.6-3 Stress in the implant along the x direction

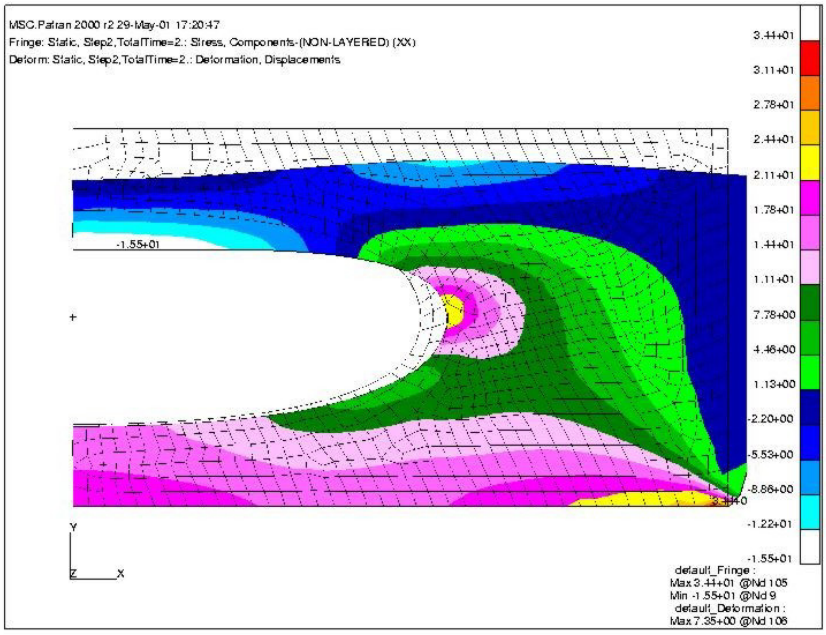

Figure 3.2.4.6-4: Stress in the tissue along the x direction

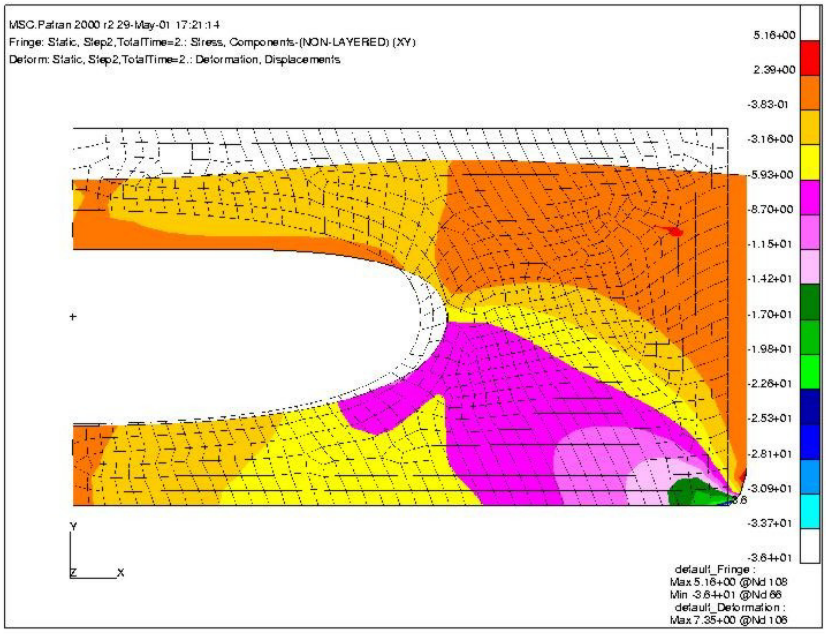

Figure 3.2.4.6-5: Shear stress in the tissue in the x-y plane

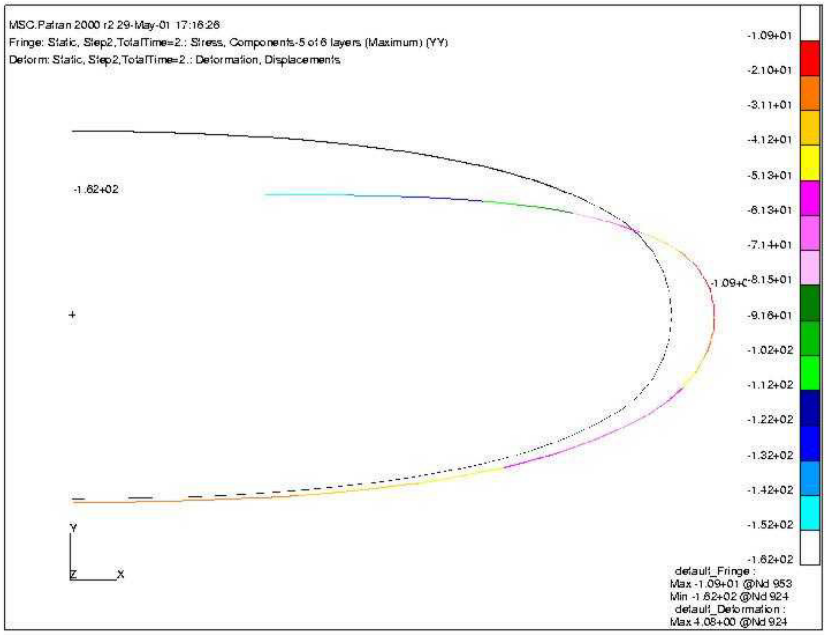

Figure 3.2.4.6-6 Stress in the implant along the y direction

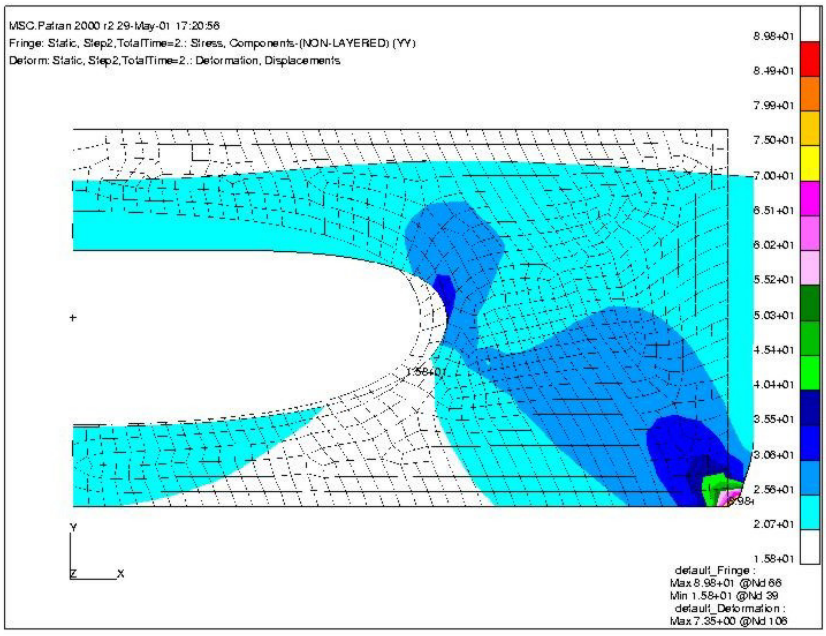

Figure 3.2.4.6-7: Stress in the tissue along the y direction

3.2.5 Nonlinear implant and tissue material models, with nonlinear geometry and a right side displacement constraint

3.2.5.1. Specific Initial Geometry

The initial geometry for this model is identical to the three previous non folded implant and tissue models. The implant was parabolic, while the tissue fills the block out so that the initial geometry is the same as in the linear tissue and implant model.

3.2.5.2. Specific Material Models

Both the tissue and the implant material formulations in this model are the nonlinear material models for the tissue and the implant. This means that this models base models and geometry are identical to the nonlinear implant and tissue without the right side constraints.

3.2.5.3. Specific Boundary Conditions

The base of this model is constrained in both the x and y directions, the right side of the model is allowed to move freely in the y direction, but is constrained such that there is no motion in the x direction. The top of this model has a distributed load in the vertical direction, with no displacement constraint in either the x or y directions. The left side of the tissue and the two leftmost nodes of the implant have the axisymmetric boundary condition applied to them, which allows for motion in the y direction, but not in the x direction. The fluid pressure was set to 0 kPa (0 psi) before the external load on the tissue was applied.

3.2.5.4. Specific Component Interactions

The interactions that are present in this model are the contact between the tissue and the implant, and the fluid-implant interaction. The tissue–implant contact is defined with no separation and no slipping, the tissue is the master surface and the implant is the slave surface.

3.2.5.5. Specific External Loading

Distributed load, same model as other nonlinear model with exception to the right side boundary condition.

3.2.5.6. Results

There is an unknown error in this model, which taints the results. The nature of the error in the FEA model is not evident at this time, though there is a possibility of a link to the unstable material formulation in the nonlinear tissue model. This model really indicates that there is more information needed to develop the FEA models in two and three dimensions. Biaxial test data for both the breast tissue and the implant material would, as stated previously, generate more accurate FEA results.

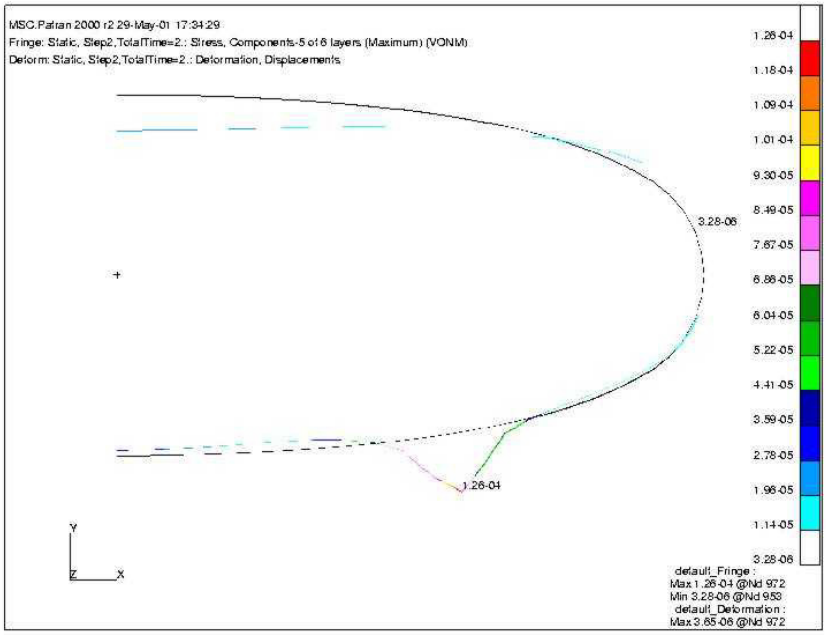

Figure 3.2.5.6-1: Von Mises in the implant stresses, note the bulge in the lower center of the implant, this is an example of an error in the model

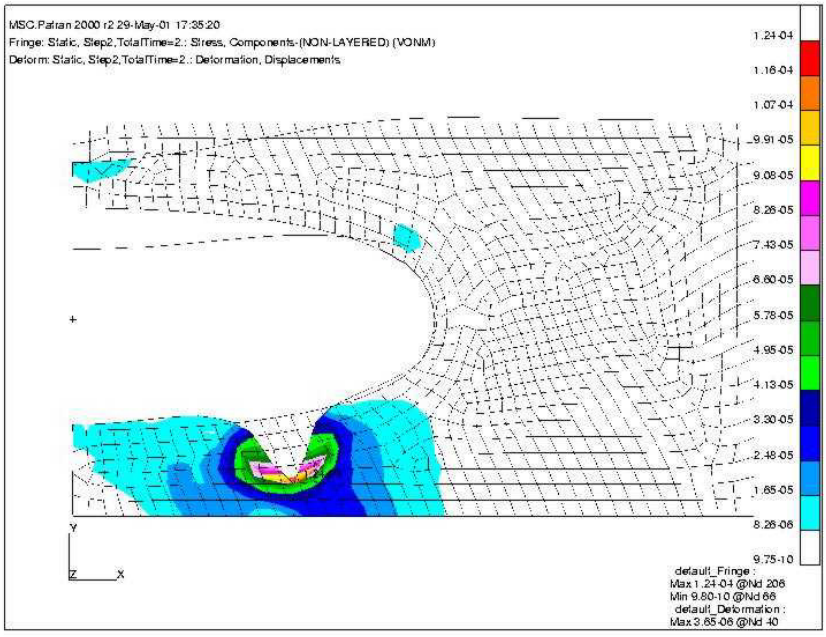

Figure 3.2.5.6-2: Von Mises in the tissue, because of the contact modeling between the implant and the tissue the bulge also appears here

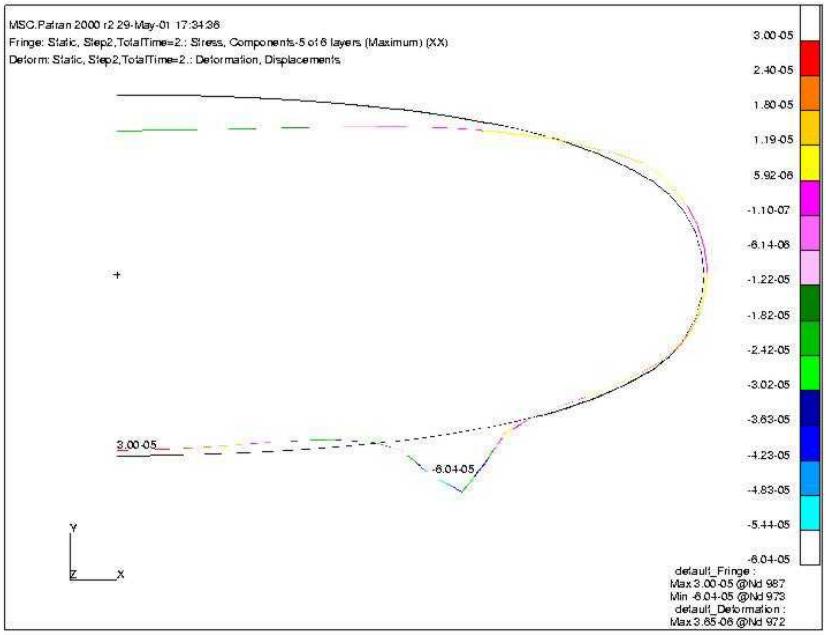

Figure 3.2.5.6-3: Stress in the implant along the x direction

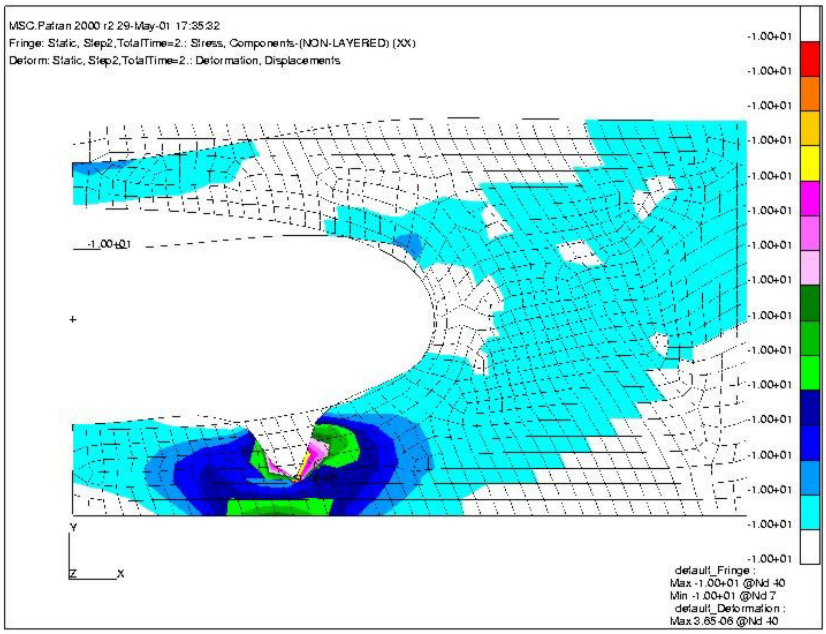

Figure 3.2.5.6-4: Stress in the tissue along the x direction

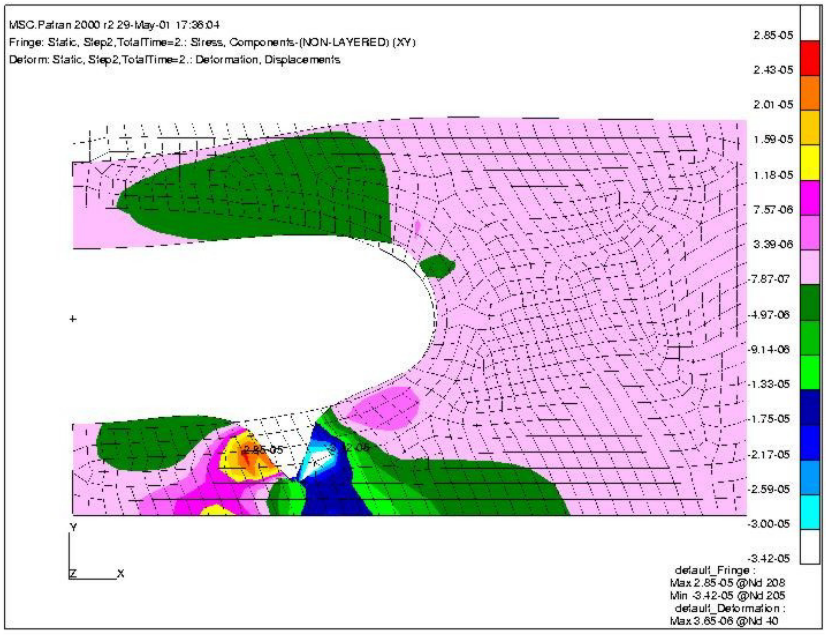

Figure 3.2.5.6-5: Shear stress in the tissue in the x-y plane

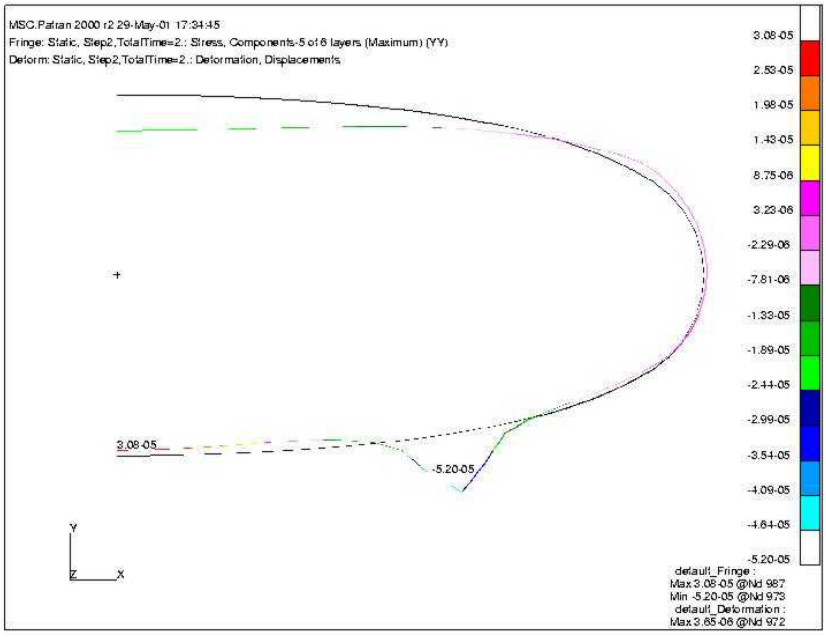

Figure 3.2.5.6-6: Stress in the implant along the y direction

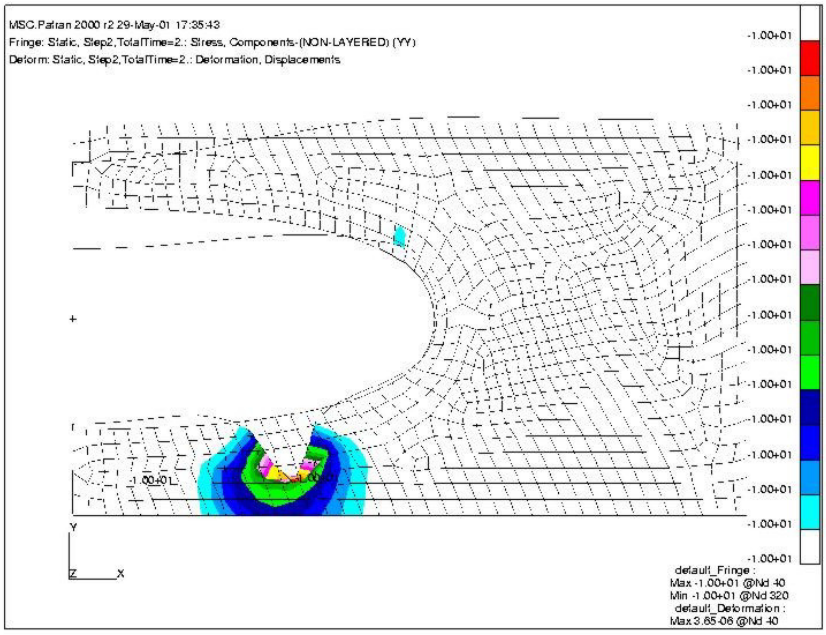

Figure 3.2.5.6-7: Stress in the tissue along the y direction

4. Fatigue Introduction:

There are three pieces of information that are required for fatigue calculations. First is the stress to number of cycles to failure (S-N) curve. Second is an estimation of the internal stresses in the object that is being analyzed given different loading configurations, in this project the internal stresses are being estimated using a finite element method (FEM) analysis. The last piece of information is the loading spectra that the object will undergo over a typical lifetime period.

4.1. Internal Stress Analysis:

The calculation of a fatigue life estimate begins with stress analysis. The FEM analysis discussed in section 3 is the basis of this internal stress analysis of the implants. Once the internal stresses are determined, the fatigue life calculation can proceed.

4.1.1 Mechanical Testing

4.1.1.1. Load and Displacement control

There are two types of control that the mechanical testing can be performed with. The first method of control is load control, the second control method is displacement control. Load control is typically used for stiff engineering materials like metals and composites. The stress amplitude and mean stress is constant in the test specimen throughout the life of the test, the strain throughout the specimen is not constant in a load controlled test. The stress in the specimen is determined through the axial stress equation $\sigma = \frac{P}{A}$, where P is the axial load and A is the cross-sectional area of the specimen.

Displacement control is typically used for less stiff materials like rubber and polymers. The stress in the specimen is not constant through the entire fatigue test, the strain throughout the specimen is kept constant for the duration of the test.

4.1.1.2. Development of the S-N Curve

The first requirement for the development of the stress vs. number of cycles to failure (S-N) curve is that the testing method matches the mechanical loading that is seen in the service life of the implant. Developing the S-N curve requires that the material be tested at enough stress levels that the curve is both smooth and contains all significant information including the fatigue limit. Multiple test specimens need to be tested at each stress level so that a statistical average is generated for each of the points on the S-N curve. The S-N curve for a material is a way of displaying the information from the fatigue tests. The information in the S-N curve is used in conjunction with the loading spectra to generate a fatigue life estimate. This is done using the Palmgren-Miner Rule.

4.1.1.3. Testing using the Load Spectra Directly

The loading spectra can be used for fatigue testing of any object. The first problem with this method of testing is that the basis of information that is built about the material is lost when a minor change to the geometry is made. The problem with this fatigue life generation method is that it assumes that the loading spectra that is being tested to is correct and will not change due to more accurate loading information.

4.1.2 Loading Spectrum Estimation

The loading spectrum estimation is key for the calculation of the fatigue life. The loading spectra can be used for either fatigue life calculation based on the S-N curve or fatigue testing of the object on the entire object. The loading spectrum needs to be as accurate as possible, so that no matter which fatigue testing method is used the results of the test are correct.

4.1.3 Technical Data about Fatigue Life Estimation

To accurately generate a fatigue life for implant material, the first step is the completion and verification of both the two-dimensional and three-dimensional FEA models. Then the fatigue testing needs to be conducted, with the S-N curve for the implant material being fully defined, including the location of the fatigue limit. The third step to calculating the fatigue life of the implants is the generation of a load spectrum. Finally, the S-N curve and the loading spectrum should be used in the Palmgren-Miner rule for the calculation of the fatigue life.

4.1.4 S-N Curve

The stress amplitude of the test is plotted on the ordinate axis of the plot, while the number of cycles that were required to reach a designated failure are plotted on the abscissa of the plot. One point is plotted for each fatigue test that is run. The curve that best fits through the test data determine the S-N curve for the material.

4.1.5 Loading Spectra and Cycle counting

Once the loading spectrum is defined, a rainflow cycle counting technique needs to be applied, for that all the information about the loading spectrum is available for the fatigue life estimation using the Palmgren-Miner Rule. All stress histories consist of peaks and valleys and the rainflow cycle counting method takes advantage of these peaks and valleys for cycle counting and ultimately for the estimation of the fatigue life. The ranges between the peaks and valleys are used to determine the stress amplitude of each cycle. Peaks and valleys that are immediately next to each other are referred to as a simple range. Peaks and valleys that are not next to each other are overall ranges. A single range is determined to be a single cycle, the information for each cycle is inserted into the Palmgren-Miner Rule, for the estimation of the number of cycles to failure.

4.1.6 Palmgren-Miner Rule

The Palmgren-Miner rule is the final step in determination of the fatigue life. The damage ratio for the breast implant is calculated for each stress, N_j is the number of cycles that occur in the loading spectra at a given internal stress level. N_{fj} is the number of cycles to failure at the same stress level determined from the S-N Curve. The form of the Palmgren-Miner rule is $B_f\left[\sum \frac{N_j}{N_{f_j}}\right]_{\text{one rep.}} = 1$, where B_f is the number of loading cycles that occur before the failure as a whole number, $\frac{N_j}{N_{f_j}}$ is the damage ratio of the material determined from the S-N Curve for a single stress level.

4.2. FEA Conclusions

There is a need to develop the S-N curve and the loading spectra if there is a desire t compute a fatigue estimate for the saline filled mammary prosthesis. There are many possible results, but the result that is most likely is that by and large the implants have very long fatigue lives. The final area that needs to be looked into for the fatigue analysis is the possibility that damage is done to the implants during the implantation process. There is a relationship between the size of the incision on implantation and the failure rate of the implants during the first year [Reference 2]. These failures would occur during what would be considered the break-in period for the implants. Failures during the break-in period typically points to a variability in quality control, in the case of the implants that were examined for this research there appeared to be consistent quality in the implants. If there is consistent quality when the implants leave the manufacturing process, then the variability of implantation installation procedures is the next place to look. Because the implantation of the implants maybe reducing the effective fatigue life of the implants. This means that the fatigue life before implantation as well as after implantation needs to be investigated.

5. Conclusions

Most of the results are placed under each individual model description. There were two specific conclusions that need to be identified. The first conclusion is the compressive stress arises at the right side of the implant. The second major conclusion was the possibility that a buckling would be the primary failure mechanism. Other conclusions include the need for more biaxial tissue material formulations, determining the validity of assumptions in the FEA models, and the need for the development of true three-dimensional FEA models for dynamic analysis.

The compressive stresses at the right side of the implant are consistent with the answers that were achieved in the previous research [Reference 3]. Though the determination that these stresses were compressive has changed the way the implants need to be tested and analyzed, overall the modeling techniques do not need require revision. The implant design should be modified to consider the compressive stresses at this boundary. There is a possibility that some of the assumptions in this work are not completely correct, however, with more research the validity of the assumptions can be easily determined.

The possibility of buckling in the implants is significant, as a thin shell, similar to the shell of the implant, has very little resistance to buckling. Thickening the implant walls or incorporating thin ribs could counteract this lack of bending rigidity; both of these changes would stiffen the implant walls with respect to bending moments. Both of these possibilities, as well as any other design change should be investigated utilizing three-dimensional FEA models.

The tissue material formulation needs to be perfected before the FEA analysis should be completely trusted. The tissue material formulation used in this analysis was unstable. It is suggested that the mammary tissue needs to be mechanically tested. Then the power laws or exponential laws describing the behavior could be worked out. This information would then need to be inserted into the FEA code. The estimates that were generated in this project show that the FEA models, if given the correct information, will produce accurate results. This conclusion starts to show both the complications and the success of this project. The lack of a mechanically tested tissue material formulation could create some error in the FEA results, but with a proven tissue material formulation the FEA results should be completely correct.

There are other FEA errors that have not been totally eliminated, the primary example of this is in the nonlinear implant and tissue models with a right side constraint. It is possible that this error comes from the nonlinear tissue material formulation, but the true reason for this error is not known at this time.

Throughout the research there were several attempts at developing working three-dimensional FEA models. None of the three dimensional modeling was completely successful, though some advancement was made. All of the modeling attempts began with modeling the implant shell with the tissue added after some preliminary computational testing. Because the implant-only finite element models did not generate a solution the surrounding tissue was not added. It is believed that the implant-only models were not properly constrained without the tissue. It is also important to state that for any buckling analysis to be performed, a full three-dimensional model must to be developed.

Overall, the two dimensional models have led to a large body of data on the design and internal stresses of the implant shells. However, the information is not complete, and without the three-dimensional models and mechanical fatigue testing, no fatigue life calculations can be completed.

References:

Bronzino, Joseph D. (1995). The Biomedical Engineering Handbook. Chapter 19: Constitutive modeling of biologic materials by Jafar Vussoughi, pg 269 Florida: CRC

Saline-Filled Mammary Prosthesis Prospective Study for Mentor Corporation's Saline-Filled Mammary Prostheses Pre-Market Approval Application (#P990075) to the USFDA (approved May 10, 2000). Mentor Corporation.

Wilson, Kelly (1998). “Finite Element Analysis of Breast Implants”. Thesis, Department of Engineering Science and Mechanics, Virginia Polytechnic Institute and State University

Curriculum Vita

Tavis Potter was born on May 15, 1975 in Laramie, Wyoming. Tavis Potter received his Bachelors degree from Virginia Polytechnic Institute and State University in May 1998. While completing his masters of science he taught a fluid mechanics laboratory for one semester and the Engineering Science and Mechanics dynamics help session. He also worked in the fluid mechanics laboratory studying aerodynamics over double arc airfoils before beginning this research. At the time of the submission of this thesis he is working at SAIC supporting the navy's Manned Flight Simulator program modeling dynamical systems in pilot in the loop engineering flight simulators.